DARPA

MAFET-3

HRL LABORATORIES

UCSB

Contract N66001-96-C-8637
DARPA MAFET-III Program
Final Technical Report

GaN-Based 100 Watt Microwave Power Hot Electron MODFET

Prepared for
Air Force Office of Scientific Research
Attention: Dr. Gerald Witt
801 N. Randolph St.
Arlington, VA 22203-1977

by
David E. Grider
HRL Laboratories
3011 Malibu Canyon Rd.
Malibu, CA 90265

AFRL-SR-BL-TR-99-

0246

REPORT DOCUMENTATION PAGE

1. AGENCY USE ONLY (Leave Blank)	2. REPORT DATE	3. REPORT TYPE AND DATES COVERED
	30 SEP 99	Final Technical 30 JUL 96 – 30 JUN 99

4. TITLE AND SUBTITLE

GaN-Based 100W Microwave Power Hot Electron MODFET

5. FUNDING NUMBERS

N66001-96-C-8637

6. AUTHOR(S)
David E. Grider

7. PERFORMING ORGANIZATION NAME(S) AND ADDRESS(ES)

HRL Laboratories, LLC
3011 Malibu Canyon Road
Malibu, CA 90265

8. PERFORMING ORGANIZATION REPORT NUMBER

9. SPONSORING/MONITORING AGENCY NAME(S) AND ADDRESS(ES)
Air Force Office of Scientific Research
801 North Randolph Street, Room 732
Arlington, VA 22203-1977

10. SPONSORING/MONITORING AGENCY REPORT NUMBER

11. SUPPLEMENTARY NOTES

12a. DISTRIBUTION/AVAILABILITY STATEMENT
Distribution Statement A. Approved for public release; distribution is unlimited.

12b. DISTRIBUTION CODE

13. ABSTRACT (maximum 200 words)

Under this program, the HRL/UCSB team has demonstrated GaN MODFET devices with microwave power densities at X-Band and K-Band frequencies that are several times larger than conventional solid state microwave power devices such as GaAs-based PHEMTs. The results of this program form the basic foundation for the development of a GaN MODFET technology capable of revolutionizing the field of microwave power electronics.

The HRL/UCSB team has developed the essential elements for a GaN MODFET microwave power device technology including both MBE and MOCVD material growth, a 0.25 μm gate length GaN MODFET fabrication process, as well as an integrated heat-spreader/flip-chip approach to thermal management.

MBE-grown GaN MODFET devices with excellent and highly uniform (i.e., variation ~ 4 % across a 2-in. wafer) DC and small signal RF characteristics have been demonstrated. In addition, the first MBE GaN MODFET capable of producing 1 Watt of microwave output power at a frequency of 8 GHz has been demonstrated under this program. MOCVD GaN MODFETs have also been developed which exhibit very high microwave output power densities of up to 3.3 W/mm and a total powers of 1 Watt at a frequency of 8 GHz. MOCVD GaN MODFET devices have also been demonstrated with very high microwave output power densities of over 3 W/mm at a frequency of 18 GHz.

14. SUBJECT TERMS

15. NUMBER OF PAGES

16. PRICE CODE

17. SECURITY CLASSIFICATION OF REPORT	18. SECURITY CLASSIFICATION OF THIS PAGE	19. SECURITY CLASSIFICATION OF ABSTRACT	20. LIMITATION OF ABSTRACT
U	U	U	U

Table of Contents

I. Executive Summary

GaN-based Modulation Doped Field Effect Transistor (GaN MODFET) technology has the potential to dramatically impact a broad range DOD-vital systems which utilize microwave power electronics at X-Band frequencies and higher /1/. Under this program, the HRL/UCSB team has demonstrated GaN MODFET devices with microwave power densities at X-Band and K-Band frequencies that are several times larger than conventional solid state microwave power devices such as GaAs-based PHEMTs /1-7/. The results of this program form the basic foundation for the development of a GaN MODFET technology capable of revolutionizing the field of microwave power electronics.

The HRL/UCSB team has developed the essential elements for such a GaN MODFET technology including material growth, device fabrication, thermal management, and device characterization. Under this program, excellent quality GaN MODFET heterostructure device material has been successfully grown using both Molecular Beam Epitaxy (MBE) and Metal-Organic Chemical Vapor Deposition (MOCVD) material growth techniques. A 0.25 μm gate length GaN MODFET fabrication process has been developed which is capable of producing microwave power devices operating at frequencies from X-Band up to K-Band frequencies. Integrated into this fabrication process is a unique heat-spreader/flip-chip thermal management approach which addresses the critical issues associated with self-generated heating which can ultimately limit the performance of GaN MODFET microwave power devices.

Using GaN MODFET heterostructure device material grown by MBE directly on sapphire or on GaN template material (i.e., GaN grown on sapphire by MOCVD), the HRL/UCSB team has demonstrated GaN MODFETs with excellent DC and small signal RF characteristics /1,5-6/.

These 0.25 μm MBE GaN MODFETs exhibit excellent device uniformity (i.e., variation ~ 4 % across a 2-in. wafer) which is comparable to more conventional and well-established GaAs- and InP-based FET technologies. Under this program, the HRL/UCSB team has also demonstrated the first MBE GaN MODFET capable of producing 1 Watt of microwave output power at a frequency of 8 GHz /7/. These MBE GaN MODFETs exhibited microwave power densities of up to 1.3 W/mm at this frequency.

The HRL/UCSB team has also developed 0.25 μm MOCVD-grown GaN MODFETs with extremely high power densities at X-Band and K-band frequencies under this program /2-4/. MOCVD GaN MODFETs have been demonstrated with microwave output power densities of 3.3 W/mm at a frequency of 8 GHz. MOCVD GaN MODFET devices capable of producing up to 1 Watt of microwave output power at 8 GHz have also been demonstrated. In addition, MOCVD GaN MODFET devices have been developed which exhibit microwave output power densities of 3.05 W/mm at a frequency of 18 GHz.

All of these results point to the successful development of a very high performance GaN MODFET microwave power device technology under this program. As a result, this program has provided the basic foundation for the development of a high performance GaN MODFET technology.

I. Introduction

GaN-based Modulation Doped Field Effect Transistor (GaN MODFET) technology has the potential to revolutionize the field of microwave power electronics /1-34/. This will have a dramatic impact on a broad range of DOD-vital systems including future generation airborne radar systems as well as advanced satellite communications systems.

Many next generation airborne radar systems currently being developed are based on phased array radar technologies involving hundreds or more elements, each of which requires a separate T/R module with appropriate phase shifting to electronic steer the resulting radar beam. In order to effectively implement such phased array airborne radar systems (e.g., at X-Band frequencies), it is essential to develop high-performance/low-cost solid state High Power Amplifiers (HPAs), which are critical components of T/R modules. PHEMT technology currently utilized in these systems suffers from low yield, and therefore high cost, because of long gate peripheries (e.g., 20 mm or longer), as well as reduced efficiency and power due to excessive power combining losses for the several PHEMTs required for each HPA.

GaN MODFET microwave power technology has the potential for RF output power densities that are five to ten times higher than that typically demonstrated for reliable PHEMT devices /1/. In fact, GaN MODFETs with power densities of over 3 W/mm at X-Band and K-Band have been demonstrated under this program /1-7/. Such a dramatic increase in power density means that fewer GaN MODFET devices, each having a much smaller gate periphery, will need to be power combined to build a microwave HPA with a given output power than that required using PHEMT devices, for example. In addition, scaling such higher power density GaN MODFETs to even

larger gate peripheries also opens the possibility for developing even higher total power HPAs with improved gain and efficiency.

In addition to airborne radar applications, GaN MODFET technology has the potential to significantly impact future satellite communications systems. This GaN MODFET technology should offer tremendous advantages for satellite communication transponders at Ku-, K-, Ka-Bands and potentially higher frequencies. Both Low Earth Orbit Satellite (LEOS) and Medium Earth Orbit Satellite (MEOS) system architectures will likely include phased array communications antennas with requirements for large numbers of T/R modules and high efficiency HPAs in order to electronically reorient the beam to specific areas on Earth (e.g., areas of high population).

II.A. Program Overview

The purpose of this program was to develop a GaN-based Modulation Doped Field Effect Transistor (GaN MODFET) microwave power device technology for use at X-Band frequencies. In order to advance the state-of-the-art in GaN MODFET microwave device technology, critical issues related to material, fabrication, device design, and thermal management were addressed. The ultimate goal of the baseline portion of this program was to demonstrate a GaN MODFET microwave power device capable of producing 10 Watts of output power at X-Band.

The technical approach for this program was based on the use of both MBE and MOCVD to grow the GaN MODFET heterostructure material on sapphire substrates, which is discussed in Sections III.A. and III.B. A 0.25 μm gate length GaN MODFET fabrication process, outlined in Section III.C., was developed to fabricate microwave power devices capable of operation at X-Band and higher frequencies. This GaN MODFET fabrication process included a novel heat-

spreader/flip-chip approach, which is presented in Section III.D., in order to address the critical issue of thermal management in these very high power microwave devices.

MBE-grown GaN MODFETs fabricated using this process were evaluated for their DC and small-signal RF performance. This device performance for GaN MODFETs grown by MBE directly on sapphire substrates and by MBE on GaN template material is discussed in Sections IV.A. and IV.B., respectively. The microwave power performance of MBE GaN MODFETs at X-Band frequencies was measured as presented in Section IV.C. The microwave power performance of MOCVD-grown GaN MODFETs was also measured at both X- and K-Band frequencies as discussed in Section V.

II.B. Key Device Issues for Microwave Power Devices

There are a number of key device issues that are critical factors in determining the performance of a microwave power technology including: 1) output power; 2) efficiency; and 3) gain. Many of these issues are directly related to the basic properties of the semiconductor materials used to fabricate such devices. In order to better understand the advantages of GaN MODFET device technology for microwave power electronics, it is important to examine these device issues, and the corresponding materials properties that impact them.

Output power is a key element defining the performance of a microwave power device technology. The essential device parameters controlling the output power of a field effect transistor (FET) are shown in the typical I-V characteristics for a GaN MODFET displayed in Figure 1. Under Class A operation, the transistor operates about some bias point along the idealized load line, moving between the minimum drain voltage (V_{dmin}) and maximum drain voltage at pinchoff (V_{dmax}), and the corresponding maximum (I_{dmax}) and minimum (I_{dmin}) drain currents.

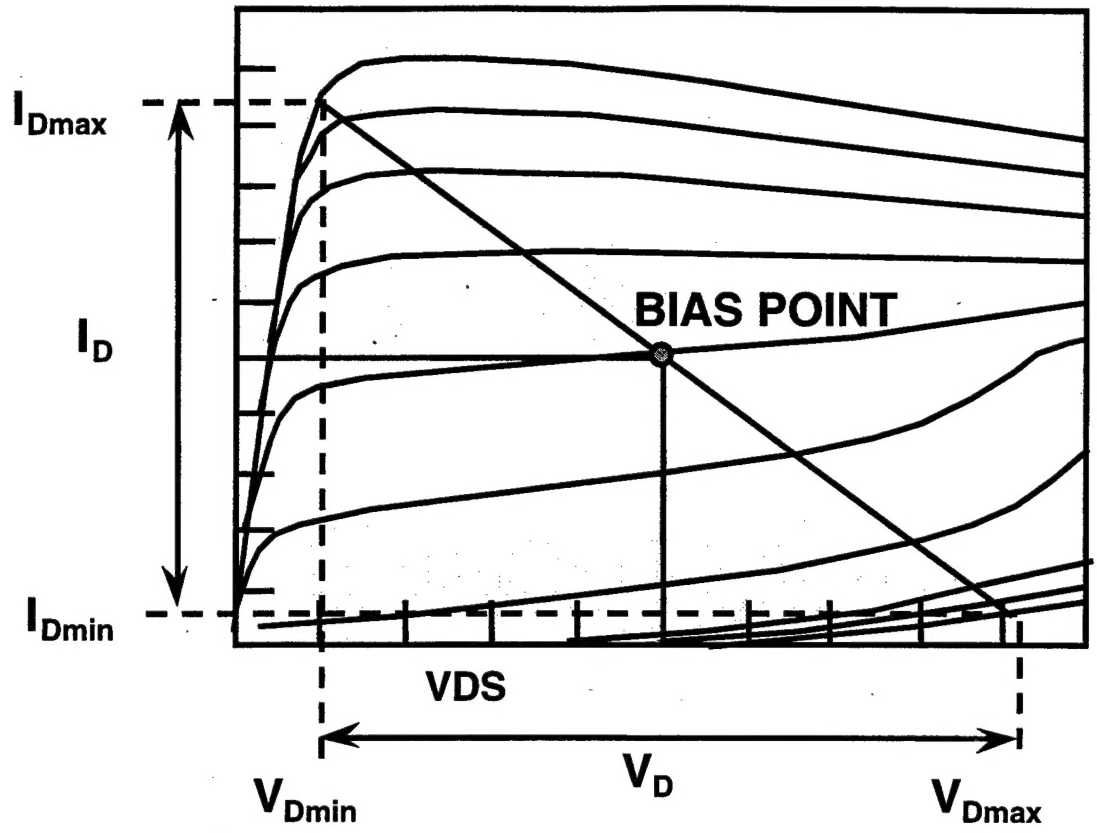

Figure 1. DC I-V characteristics for a typical GaN MODFET.

In order to maximize RF output power, therefore, it is necessary to achieve the largest possible difference between the maximum (V_{dmax}) and minimum (V_{dmin}) drain biases along with the largest possible difference between the maximum (I_{dmax}) and minimum (I_{dmin}) drain currents under RF drive. The maximum RF output power ($P_{out\text{-}max}$) is given by:

$$P_{out\text{-}max} = 1/8\ (V_{dmax} - V_{dmin})\ (I_{dmax} - I_{dmin}) \qquad \text{Eq. 1}$$

As can be seen in Figure 1, the minimum drain voltage (V_{dmin}) is determined by the knee voltage of the device I-V characteristics at the maximum drain current (I_{dmax}). The maximum drain voltage (V_{dmax}) is limited by the gate and drain bias conditions at which breakdown begins to occur, typically between the gate and drain. Above this gate-to-drain breakdown voltage (BV_{gd}), substantial gate leakage currents lead to significant degradation of the power performance of the device.

I_{dmax} is determined by the channel doping in a SiC MESFET and by the two-dimensional electron gas density (2-DEG) in a GaN MODFET device. I_{dmin} is basically determined by the pinch-off characteristics of the transistor at high drain biases near V_{dmax}. For low I_{dmin}, the device should remained pinched-off completely out to V_{dmax}. Therefore, the device characteristics needed for the highest maximum RF output power ($P_{out\text{-}max}$), are: 1) high breakdown voltage; 2) low knee voltage; 3) large drain current; and 4) good pinchoff.

Efficiency is another key element in determining the performance of a microwave power device technology. Specifically, the Power Added Efficiency (PAE) is defined as:

$$PAE = (P_{out}/P_{DC})\,(1 - 1/G) \qquad \text{Eq. 2}$$

where P_{out} is the RF output power of the device and P_{DC} is the DC power input to the device. Clearly increased large signal gain (G) results in improved PAE. This is particular important at higher microwave frequencies where gain becomes an issue.

II.C. Material Advantages of GaN MODFETs for Microwave Power

The superiority of GaN MODFET technology for solid state microwave power electronics applications is a direct result of materials properties of GaN compared with other potential high power semiconductor materials as shown in Table 1. Indeed, GaN ranks either first or second for every materials property critical to high microwave power devices. This combination of exceptional power-related materials properties makes GaN-based materials the obvious choice for microwave power electronics.

Material Properties	Si	GaAs	4H-SiC	GaN
Energy Gap (eV)	1.1	1.4	3.2	3.4
Breakdown Field (kV/cm)	300	400	1000-5000	3500
Peak Velocity (10^7 V/cm)	0.8	2	2	2.7
Mobility (cm^2/V-s)	~ 1000	~ 5000	~ 200	~ 1500
Thermal Cond. (W/cm-K)	1.5	0.5	5	1.3
Dielectric Constant	11.9	12.8	9.7	9
Johnson - Figure of Merit	1	11	410	790

Table 1. Comparison of widegap and conventional semiconductor materials relevant to microwave power device technologies.

Another significant advantage of GaN-based materials for microwave power devices is the ability to fabricate heterostructure devices such as $Al_xGa_{1-x}N$/GaN MODFETs. As will be discussed in more detail in the following section, such devices offer significant performance advantages for microwave power applications at X-Band frequencies and higher.

The large breakdown field of GaN represents one of the key advantages of this material for microwave power devices. The large breakdown field of GaN (3500 kV/cm) compared with that

of Si and GaAs (300 kV/cm and 400kV/cm, respectively) is associated with the significantly larger bandgap (E_g = 3.4 V) of GaN. As is the case with SiC, which also has a large breakdown field (i.e., 1000 to 5000 kV/cm), this means that GaN-based devices can be operated at significantly higher device operating voltages. This increased voltage swing, in turn, leads directly to dramatically higher microwave output powers for such devices.

Electrical transport properties in these semiconductor materials is particularly relevant for devices designed to operate at X-Band frequencies (i.e., 7 to 11 GHz) and higher. Although the electron mobility in bulk GaN (1500 cm^2/V-S at an electron concentration of 1 X 10^{17} cm^{-3}) is substantially lower than that in bulk GaAs (5000 cm^2/V-S), it is several times larger than that of 4H-SiC material (200 cm^2/V-S). It should be noted, however, that electron mobility plays a somewhat less important role in field-effect transistor (FET) microwave power devices than might be expected. This is due to the very large drain biases present in such devices which give rise to very large electric fields along the channel. As a result, electrons in the channel are quickly accelerated through the low-field mobility portion of the velocity-field curve to significantly higher velocities.

Because of these very large electric fields along the channel of the device, however, the electron peak velocity actually plays a much more important role than electron mobility in determining the performance of FET microwave devices at the higher microwave frequencies. As shown in Table 1, GaN exhibits the highest peak velocity (V_{pk} = 2.7 X 10^7 /cm^2) of all the semiconductor materials shown. Indeed, it is 35% higher than the next highest value of V_{pk} = 2.0 X 10^7 /cm^2 exhibited by GaAs and 4H-SiC and is over three times higher than that of Si. The extremely high electron peak velocity in GaN offers the potential for GaN-based microwave power devices with substantially improved high frequency performance (i.e., higher f_T and f_{max})

and enhanced efficiency. It is somewhat fortuitous that GaN material exhibits a very large breakdown voltage which makes it possible to take advantage of the high electron peak velocity in this material, leading to GaN MODFET devices with enhanced gain and efficiency at X-Band frequencies and higher.

The dielectric constant of GaN is lower than that of 4H-SiC and is substantially lower than that of either Si or GaAs. This means that any capacitances in the device, such as the gate-to-drain capacitance, will be smaller in GaN-based transistors than in those based on these other semiconductor materials. In general, these reduced capacitance values will, in turn, result in improved device performance. For example, the reduction in gate-to-drain capacitance in GaN MODFETs will result in higher values for the unity current gain cut-off frequency (f_T).

The ultimate performance of solid state devices based upon different semiconductor materials can be compared using a quantity known as the Johnson Figure of Merit (JFOM) which is given by:

$$JFOM = [(E_c)(v_s)/2\pi]^2 \qquad \text{Eq. 3}$$

where E_c is the critical breakdown field and v_s is the electron saturation velocity in the material. As shown in Table 1, the Johnson Figure of Merit for GaN is roughly double that of 4H-SiC, its closest competitor. Indeed, this figure of merit for GaN is actually more than 70 times higher than that of GaAs. This is particularly relevant since GaAs-based PHEMT devices represents the current technology of choice for microwave power applications at X-Band frequencies (e.g., HPAs in T/R modules of X-Band radars).

II.D. Device Advantages of GaN MODFETs for Microwave Power

In addition to the basic materials advantages of GaN, the ability to epitaxially grow GaN-based heterostructure devices such as $Al_xGa_{1-x}N$/GaN MODFETs offers significant additional device advantages for this technology over competing microwave power technologies such as SiC MESFETs. The heterostructure device cross-section of an $Al_xGa_{1-x}N$,/GaN MODFET is shown in Figure 2. The device heterostructure, which is grown epitaxially by Metal Organic Chemical Vapor Deposition (MOCVD) or by Molecular Beam Epitaxy (MBE) on sapphire substrates, consists of an undoped GaN buffer layer and channel with an $Al_xGa_{1-x}N$ Schottky layer on top.

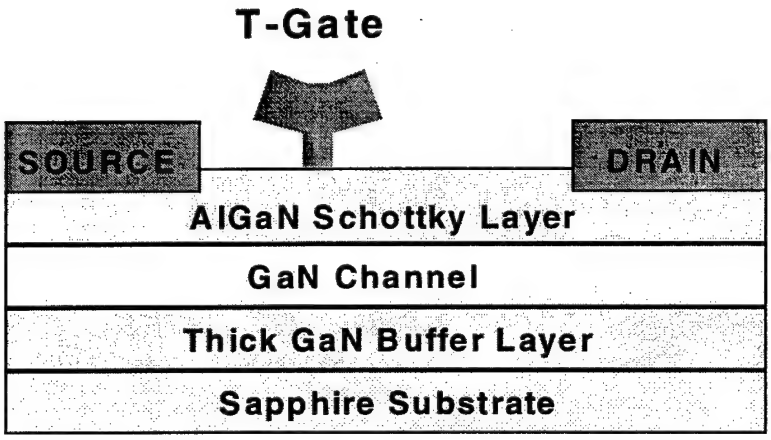

Figure 2. Typical heterostructure device cross-section for $Al_xGa_{1-x}N$,/GaN MODFET on a sapphire substrate.

Because of the presence of the wider bandgap of $Al_xGa_{1-x}N$ material above the GaN channel, a two-dimensional electron gas (2-DEG) forms in the GaN channel just below the $Al_xGa_{1-x}N$ Schottky layer. There are two possible sources of the electronic charge for this 2-DEG. First, the $Al_xGa_{1-x}N$, layer can be doped (e.g., with Si), in which case a phenomenon known as modulation

doping occurs. In this case, donor electrons are transferred in real space out of the $Al_xGa_{1-x}N$ layer, which has a wider bandgap and therefore higher conduction band, into the GaN channel, leaving the ionized Si donors behind. A second source of electrons in the 2-DEG, which occurs independent of doping, is associated with the piezoelectric charge built up in the slightly compressively strained $Al_xGa_{1-x}N$, layer /27-29/. The field resulting from this fixed piezoelectric charge results in accumulation of mobile electrons in the 2-DEG in the GaN channel layer. Both of these mechanisms, in combination with the large conduction band discontinuity between $Al_xGa_{1-x}N$, and GaN, are responsible for the very large 2-DEG sheet carrier concentration (i.e., typically $1 - 2 \times 10^{13}/cm^3$), and ultimately the large current densities (i.e., I_{dmax} up to 1 A/mm and higher) observed in GaN MODFET devices.

The spatial separation of this 2-DEG in the GaN channel from both the ionized donors and the fixed piezoelectric charge in the $Al_xGa_{1-x}N$ leads to reduced scattering from these fixed charges. This improved electron transport is reflected in the fact that GaN MODFETs, with a 2-DEG, exhibit significantly higher gain and efficiency than either a GaN MESFET or a SiC MESFET, in which there is significant ionized impurity scattering from the Si donors.

The enhanced gain of GaN MODFETs is illustrated quite clearly in Figure 3, which shows a plot of the unity current-gain cutoff frequencies (f_T) as a function of gate length obtained for different device technologies. For all gate lengths, the values for f_T in GaN MODFETs are significantly higher than those for either GaN MESFETs or SiC MESFETs. As can be seen in Figure 3, the HRL/UCSB team has demonstrated 0.25 micron gate length GaN MODFETs with f_T values of up to 50 GHz under this program. It should also be noted that the gate-to-drain breakdown voltage (BV_{gd}) of this device was over 80 Volts per micron of source-drain

separation. This combination of gain and breakdown voltage clearly indicates that HRL's GaN MODFET technology is a viable candidate for microwave power applications.

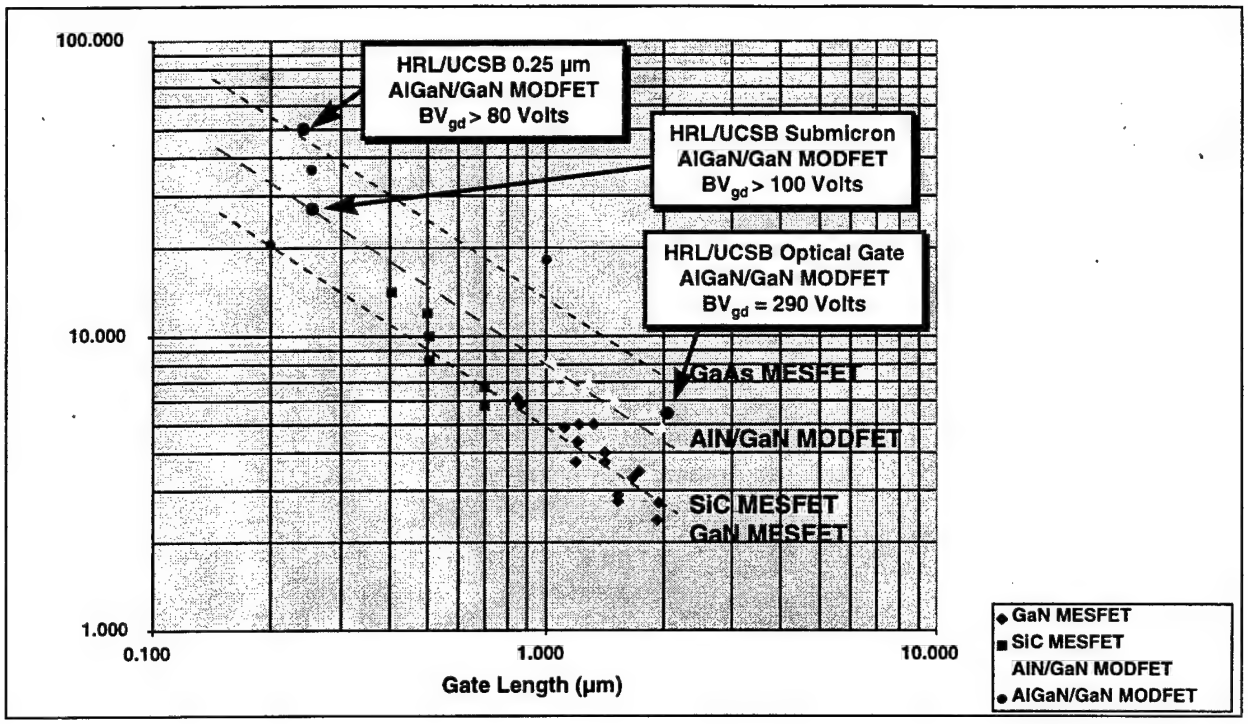

Figure 3. Unity current-gain cutoff frequency (f_T) as a function of gate length for different microwave power device technologies including GaN-based MODFETs, SiC MESFETs, GaN MESFETs and, for comparison, GaAs MESFETs.

The presence of the wider bandgap $Al_xGa_{1-x}N$, Schottky layer in the GaN MODFET device shown in Figure 2 offers the added advantage of high current density in the device as alluded to previously. The large conduction band discontinuity between $Al_xGa_{1-x}N$, and GaN results in a very high 2-DEG sheet carrier concentration (i.e., typically 1 – 2 X $10^{13}/cm^3$) in the GaN channel region just below the $Al_xGa_{1-x}N$ Schottky layer. This, in turn, results in very large current densities (i.e., I_{dmax} up to 1 A/mm and higher) in GaN MODFET devices.

Another major advantage of the $Al_xGa_{1-x}N$, Schottky layer in the GaN MODFET is that it serves to further increase the gate-to-drain breakdown voltage in these devices. Values for the gate-to-drain voltage (BV_{gd}) of 80 V and even higher are readily achieved in these devices. As discussed in the previous section, the very high gate-to-drain high breakdown voltages (BV_{gd}) in conjunction with the extremely current densities (I_{dmax}) inherent in these GaN MODFET transistors should result in microwave power transistors with very high RF output power densities.

The RF power density in SiC MESFETs is limited by the fact that there is no equivalent wider bandgap material to serve as a Schottky layer in the SiC materials system. In such SiC MESFET devices, there is a severe tradeoff between the gate-to-drain breakdown voltage (BV_{gd}) and the current densities (I_{dmax}) in the device. In order to increase I_{dmax} in the transistor , it is necessary to increase the doping in the SiC channel under the gate of the FET. At the same time, however, increased doping in this region significantly degrades the gate-to-drain breakdown voltage of the device. This tradeoff between BV_{gd} and I_{dmax} obviously limits the RF output power densities that can ultimately be achieved in these SiC MESFET devices for exactly the same reasons as discussed previously.

III. GaN MODFET Device Fabrication

The GaN MODFET fabrication process developed by HRL was designed to address the critical issues for microwave power devices outlined in Section II. The fabrication process utilizes GaN MODFET device heterostructures grown using either Metal-Organic Chemical Vapor Deposition (MOCVD) or Molecular Beam Epitaxy (MBE) which will be discussed in Sections III.A and III.B. The basic device fabrication portion of the process, which is outlined in Section III.C., utilized electron beam lithography to fabricate the relatively short (i.e., 0.25 μm) gate length GaN MODFET devices. The heat-spreader/flip-chip approach for thermal management, which is outlined in Section III.D., is a crucial element of the fabrication process due to the very large power densities achievable using this GaN MODFET technology.

III.A. GaN MODFET Materials Growth

Under this program, the HRL/UCSB team has used both Molecular Beam Epitaxy (MBE) and Metal-Organic Chemical Vapor Deposition (MOCVD) to grow GaN MODFET heterostructure device material. The baseline approach under this program involved either MBE or MOCVD growth of GaN MODFET device heterostructures directly on sapphire substrates such as that shown in Figure 4. During the course of this program, a hybrid approach was also investigated involving MBE regrowth of GaN MODFET heterostructures on GaN template material previously grown on sapphire by MOCVD. Because the GaN MODFET device heterostructure varied with individual devices fabricated under this program, the details of these heterostructures will be presented with the device performance results in Sections IV and V.

The defining characteristic of both MBE and MOCVD growth of GaN MODFET device heterostructures is the extremely large lattice mismatch between the GaN epilayer material and

the sapphire substrate on which it is grown. There is a 14% lattice mismatch between the GaN hexagonal Wurtzite phase (a = 3.180 Å, c = 5.166 Å) and the basal plane of sapphire (a = 4.755 Å, $a/\cdot\sqrt{3}$ = 2.748 Å, c = 12.991 Å). This enormous lattice mismatch unavoidably leads to very high misfit dislocation densities. Indeed, threading dislocations densities in the range of 10^9 /cm^2 are typically observed in these films. This mismatch also tends to promote three-dimensional island growth of the GaN. As a result, the nucleation of GaN growth on sapphire is a critical step for both MOCVD and MBE. Both techniques utilize a thin GaN nucleation layer that is grown at substrate temperatures well below normal. The GaN buffer and GaN MODFET device structure is then grown subsequently at higher substrate temperatures.

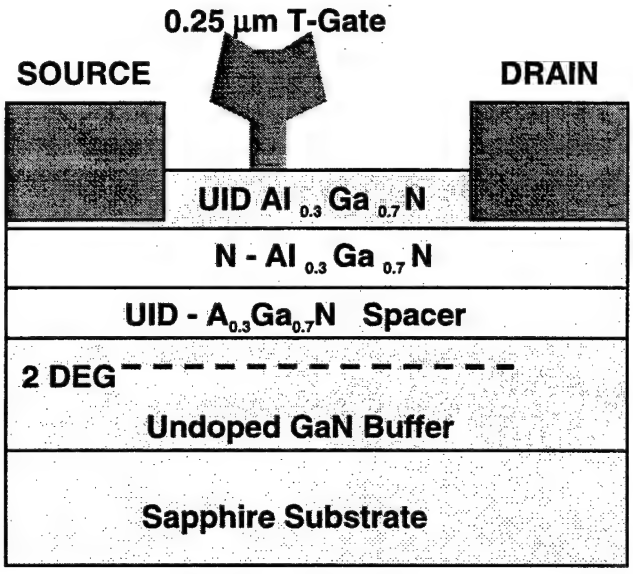

Figure 4. $Al_xGa_{1-x}N$/GaN MODFET device heterostructure grown using MBE on a sapphire substrate.

The MOCVD growth of GaN MODFET device heterostructure materials was carried out using a horizontal flow atmospheric reactor operated at atmospheric pressure. Trimethylgallium

(TMGa), Triethylaluminum (TEA), and Ammonia (NH_3) were used as precursors for the group-III and group-V species, and Si n-type doping was accomplished using disilane. After annealing the sapphire substrates at 1050 °C, a thin (i.e., approximately 200 Å) GaN nucleation layer was grown at 600 °C. The substrate temperature was then raised to between 1000 °C and 1100 °C for the remainder of the growth of the GaN MODFET heterostructure.

GaN MODFET device heterostructures were also grown by MBE using a nitrogen RF plasma source for the group V species, and solid-source Knudsen cells for the Ga and Al group III species, as well as the Si n-type dopant. Following an anneal of the sapphire substrate under a nitrogen flux from the RF plasma source, the growth on the sapphire substrate was initiated using a 200 Å thick GaN nucleation layer grown at a low substrate temperature. The remainder of the GaN MODFET heterostructure was grown by MBE at a substrate temperature of approximately 600 °C.

III.B. Comparison of MOCVD and MBE Growth of GaN MODFET Heterostructures

Growth of GaN MODFET device heterostructures using MBE and MOCVD growth techniques were used under this program because each approach offers certain advantages and disadvantages. First, MOCVD growth of GaN typically has growth rates that are several times larger than that of MBE. As a result, it is much easier to grow thicker (i.e., over 1 μm) GaN buffer layers using MOCVD than it is using MBE. This is particularly important for GaN MODFET devices because increasing the GaN buffer layer thickness serves to move the active device region further away from interface between the sapphire and the initial GaN nucleation layer. One might reasonably expect, therefore, that this interfacial region would be less likely to degrade the device performance of GaN MODFETs with thicker GaN buffer layers.

A significant advantage of MBE over MOCVD in the growth of GaN MODFET device heterostructures is the significantly lower growth temperature of MBE compared with MOCVD. Because of the differential thermal expansion between the GaN-based heterostructure and the sapphire substrate upon cooling back down to room temperature following epitaxial growth, the epilayer material is under substantial strain, resulting in further dislocation formation and even cracking of the material. This phenomenon is more of an issue for the higher growth temperature MOCVD technique. Although cracking is indeed observed for MOCVD-grown GaN MODFET heterostructures with thicker $Al_xGa_{1-x}N$ Schottky layers, no such cracking is observed for equivalent MBE-grown heterostructures.

The typical temperatures for MBE growth of GaN-based heterostructures is approximately 600 °C, while those for MOCVD growth of this material is over 1000 °C. For MBE growth, the thermal expansion (i.e., $\Delta a/a_0$) of GaN and AlN perpendicular to the c-axis at a temperature of 600 °C relative to room temperature is 3.2×10^{-3} and 3.0×10^{-3}, respectively. The corresponding thermal expansion for sapphire in the direction perpendicular to the c-axis (i.e., in the basal plane) is 4.8×10^{-3}. As a result, the differential thermal expansion between the GaN-based heterostructure material and the sapphire substrate is approximately 1.6×10^{-3} for MBE-grown material.

For MOCVD growth, the thermal expansion (i.e., $\Delta a/a_0$) perpendicular to the c-axis of both GaN and AlN at 1000 °C relative to room temperature is close to 5.5×10^{-3}. The corresponding thermal expansion for sapphire is 8.7×10^{-3}, resulting in a differential thermal expansion between the GaN-based heterostructure material and the sapphire substrate of approximately 3.2×10^{-3} for MOCVD-grown material. Due to its higher growth temperature, therefore, MOCVD-grown GaN MODFET heterostructure material on sapphire experiences a tensile strain due to

differential thermal expansion that is twice as large as that of MBE-grown GaN MODFETs on sapphire, thereby leading to increased dislocation generation and cracking in MOCVD-grown material as alluded to previously.

Another advantage of MBE over MOCVD for the growth of GaN MODFET heterostructures is the significantly improved uniformity of MBE-grown heterostructure material. This leads to a dramatic improvement in the uniformity of the device characteristics of GaN MODFETs across the wafer. The increased uniformity of MBE-grown GaN MODFET heterostructure materials, and the resulting devices will be discussed in Section IV.

III.C. GaN MODFET Device Fabrication Process Flow

The submicron gate-length GaN MODFET fabrication process utilized by HRL under this program is summarized in Figure 5. The fabrication process begins with the MBE or MOCVD growth of the GaN MODFET heterostructure as shown in Figure 4 for the particular case of an MBE-grown heterostructure on a sapphire substrate.

Following the GaN MODFET heterostructure material growth, the source and drain ohmic contacts are fabricated. The source/drain contact regions are defined using optical photolithography. Next, a Cl_2 reactive ion etching (RIE) process is used to recess the source/drain contact regions through the unintentionally doped $Al_xGa_{1-x}N$ cap layer as shown schematically in Figure 4. Ohmic metal is then deposited in the recessed ohmics using a Ti/Al/Ni/Au (200/2000/400/500 Å) metallization scheme. Finally, the source/drain ohmics are sintered using a rapid thermal anneal process (RTA) at 900 °C for 30 sec.

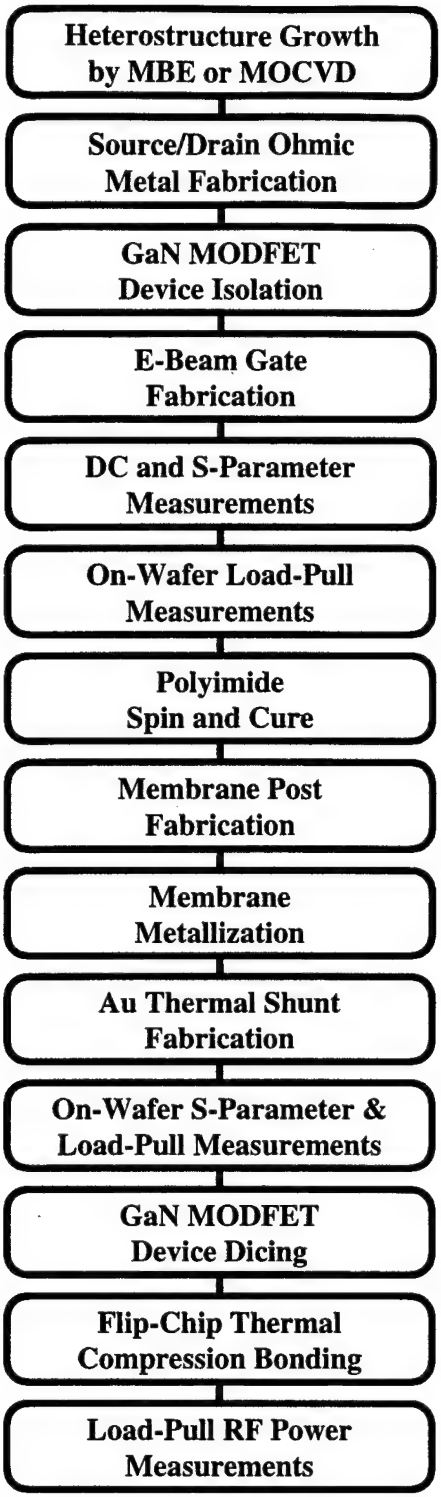

Figure 5. Process flow for the fabrication and testing of submicron gate length GaN MODFET devices including heat-spreader/flip-chip fabrication.

The next step in the fabrication process is mesa isolation of the GaN MODFET devices. The mesa isolation regions are defined using optical photolithography. A Cl_2 reactive ion etching (RIE) process is used to etch the mesas. The mesas are etched below the 2-DEG in the channel and well into the undoped and highly resistive GaN buffer layer.

Following mesa isolation, 0.25 μm T-gates are fabricated on the GaN MODFET using electron beam lithography and a Ni/Au (200/3300 Å) T-gate metallization scheme. A scanning electron microscope (SEM) photograph of a fabricated 0.25 micron gate length GaN MODFET device is shown in Figure 6. The layout of the device consists of multiple 100 μm wide fingers located between alternating source and drain pads as noted in the SEM photograph. Also noted in Figure 6 is the gate feed for the device.

At this stage of the fabrication process, the source contacts of the multifinger GaN MODFET devices are not connected together. However, it is possible to carry out DC, small-signal S-parameter, and even RF power load-pull measurements on the single-finger (i.e., 0.25 X 100 micron) and double-finger (0.25 X 200 micron) devices at this point in the fabrication process. Indeed, the capacity for device characterization at this early stage in the fabrication process is a major advantage of the source-contact-only heat-spreader/flip-chip approach utilized by HRL under this program. This makes it possible to rapidly assess the quality of the heterostructure material along with that of the ohmic, isolation, and gate fabrication processes for a given wafer.

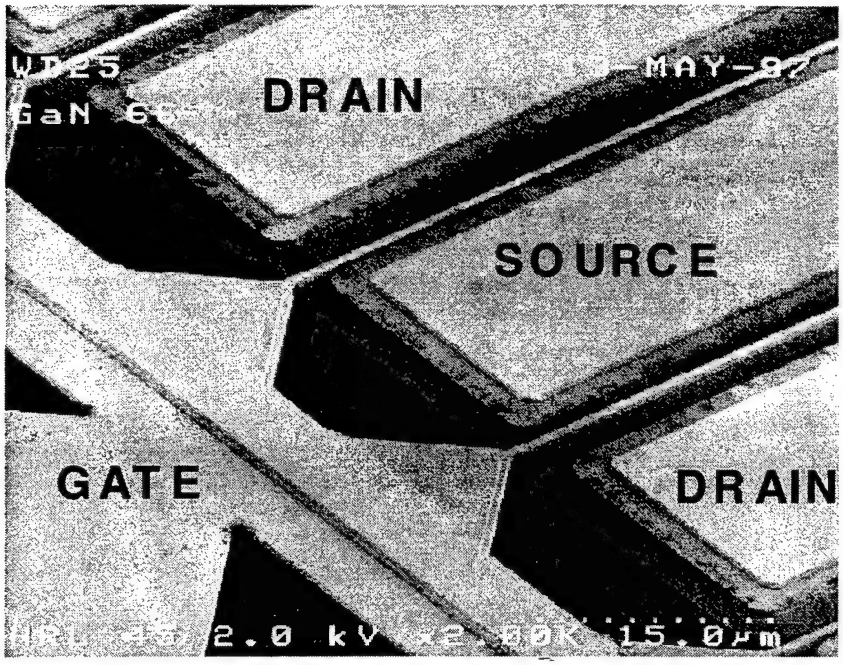

Figure 6. SEM microphotograph of 0.25 micron gate length GaN MODFET following the electron beam lithography gate fabrication step in the process.

III.D. Thermal Management Approach for GaN MODFETs

Following the characterization of the single- and double-finger GaN MODFET devices, the fabrication process outlined in Figure 5 continues with the upper level metallization steps that form the basis for the heat-spreader/flip-chip approach for thermal management in these high power devices. Thermal management is an important issue for high-performance/high-power GaN MODFETs. At an RF output power density of 10 W/mm, a device with 50% PAE must still dissipate 10 W/mm of heat, which is more than an order of magnitude higher than that of commercial GaAs PHEMTs.

HRL has developed an advanced heat-spreader/flip-chip bonding concept for the thermal management of GaN MODFETs specifically to address this issue. A major advantage of such a

heat-spreader/flip-chip approach is that it circumvents the problem of transferring waste heat from the GaN MODFET device out the backside through the substrate. This is particularly important for sapphire substrates which have thermal conductivity values that are about a factor of four smaller than that of SiC, a competing microwave power technology. An added advantage of this approach is that flip-chip bonding readily lends itself to the fabrication of low-cost MIC power amplifiers and power combining modules and can be readily extended to GaN-based MMIC power amplifiers in the future

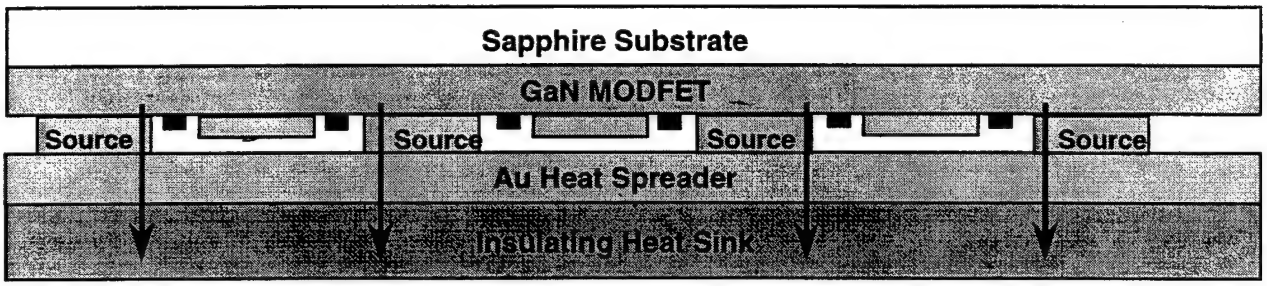

Figure 7. Schematic cross-section of heat-spreader/flip-chip approach to thermal management of GaN MODFET.

The heat-spreader/flip-chip approach utilized under this program is shown schematically in Figure 7. This approach utilizes a heat-spreader consisting of a 30 μm thick Au airbridge thermal-spreader on a polyimide support layer with posts connected to the source contacts for each finger of a multifinger wide gate periphery GaN MODFET device. This Au heat spreader serves several functions. First, it electrically connects the source pads of the multifinger GaN MODFET together. Second, it serves as a heat spreader which prevents high temperature hot spots from occurring on certain fingers of the devices by substantially reducing the thermal resistance between fingers so that the temperature distribution across the entire multifinger GaN

MODFET device is much more uniform. Finally, the thick Au heat-spreader is a key component of the subsequent flip-chip bonding of the device to a high thermal conductivity substrate such as AlN. A thermal compression bond is formed between this Au thermal-spreader layer and the contacts on the AlN flip-chip substrate.

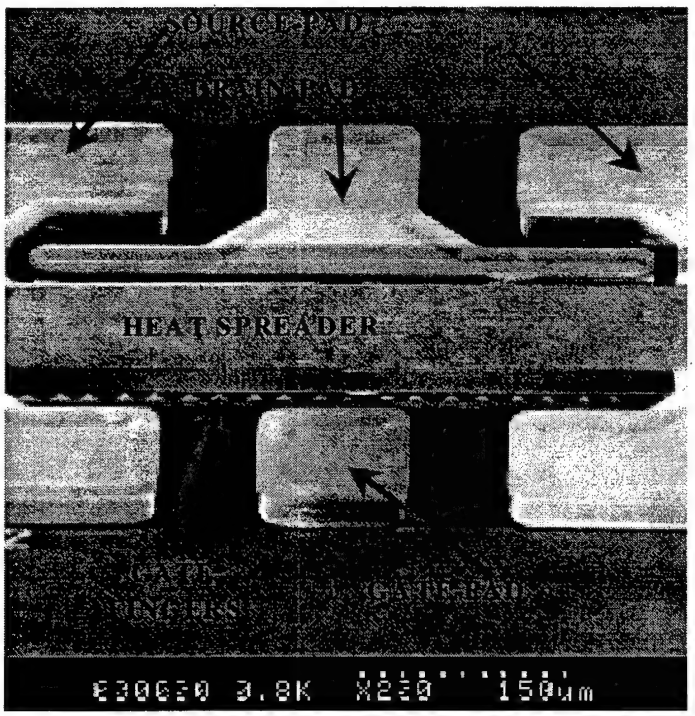

Figure 8. SEM micrographs of (a) a 20-finger test GaN MODFET (2 mm total gate periphery) with the 30 micron thick Au heat-spreader.

Continuing the GaN MODFET fabrication process flow shown in Figure 5, the initial step in fabricating the Au airbridge thermal-spreader involves spinning on and curing a polyimide support layer for the heat-spreader. This is followed by the fabrication of posts down to each of the ohmic source pads using optical photolithography. Next Au membrane metal is deposited for the span between these posts. Finally, a 30 micron thick Au thermal shunt is plated on top of this

membrane metal span, completing the Au heat-spreader fabrication. Figure 8 shows an SEM microphotograph of a 20 finger (i.e., 2mm wide) 0.25 μm gate length GaN MODFET with a completed Au heat spreader. In addition, the gate, source, and drain pads can be seen quite clearly, along with the very ends of the gate finger connections.

A significant advantage of this thermal management approach, which utilizes only the source contact to extract heat from each finger of the GaN MODFET device, is that it allows one to carry out final on-wafer DC, S-parameter, and RF load-pull power measurements on the device prior to wafer dicing and final flip-chip mounting of the device. In addition to verifying the Au heat spreader fabrication process, these final on-wafer measurements actually serve to benchmark the performance of the wider multifinger GaN MODFET devices.

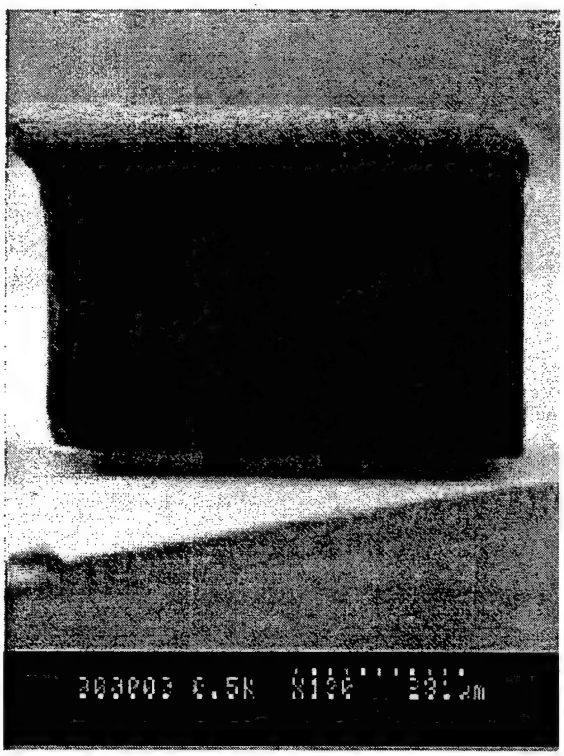

Figure 9. SEM micrographs of GaN MODFET with Au heat spreader flip-chip mounted on an substrate heat sink using thermal compression bonding.

After the individual GaN MODFET devices are diced, they are flip-chip mounted onto an AlN heat sink. A thermal compression bond is formed between the Au thermal-spreader layer and the contacts on the AlN flip-chip substrate. An SEM microphotograph of a flip-chip mounted GaN MODFET is shown in Figure 9.

Compared with an alternative approach in which both drain and source contacts are used to extract heat from the device /31/, this source-contact-only approach will inevitably result in higher channel temperatures because the heat conduction is principally through only the source contact regions of the device. However, this limitation is offset by the enhanced testability and the much less stringent requirements on lithography alignment inherent in this source-contact-only heat-spreader/flip-chip approach.

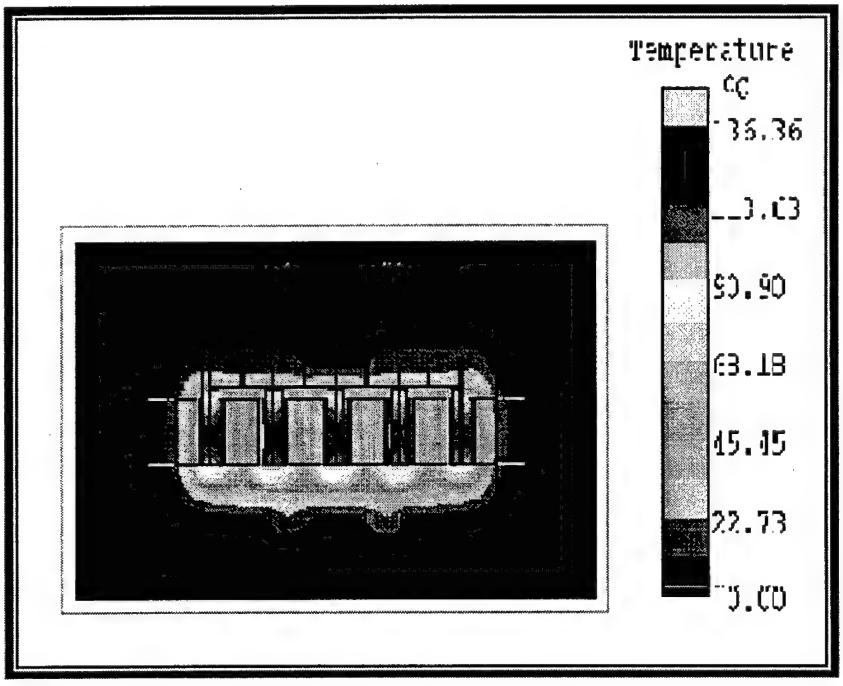

Figure 10. Temperature distribution of a 10-finger GaN MODFET at 10 W/mm dissipation obtained from finite element simulation.

HRL has carried out a finite-element thermal modeling analysis of this thermal-spreader/flip-chip thermal management approach implemented for GaN MODFETs. An example of the results of such a simulation is shown in Figure 10. This shows the temperature distribution from a 10 finger (i.e., 1 mm wide) GaN MODFET operating at 10 W/mm of power dissipation. In this simulation, the device has a 20 micron thick Au heat spreader flip-chip mounted onto an AlN substrate as a heat sink. These simulations indicate that using this thermal-spreader/flip-chip approach, the device temperature will be less than 210 °C for a power density of 10 W/mm.

IV. MBE-Grown GaN MODFET Device Performance

IV.A. MBE GaN MODFETs on Sapphire

The heterostructure for the GaN MODFET devices grown by MBE on sapphire is shown in Figure 4. The device heterostructure begins with a thin (i.e., approximately 200 Å) GaN nucleation layer grown directly on c-plane sapphire substrate, followed by a 5000 Å undoped highly resistive GaN buffer layer. The Al mole fraction was kept at x = 0.3 for the entire $Al_xGa_{1-x}N$ Schottky layer. This layer consisted of 30 Å unintentionally doped (UID) $Al_xGa_{1-x}N$ spacer layer, a 50 Å $Al_xGa_{1-x}N$ layer doped n-type with Si at 2 X 10^{19} cm^{-3}, and a 250 Å unintentionally doped (UID) $Al_xGa_{1-x}N$ cap layer. Room temperature Hall mobility measurements on these GaN MODFET heterostructures exhibited an electron mobility of 1000 cm^2/V-S at a sheet carrier concentration of 1.6 X 10^{13} cm^{-2}.

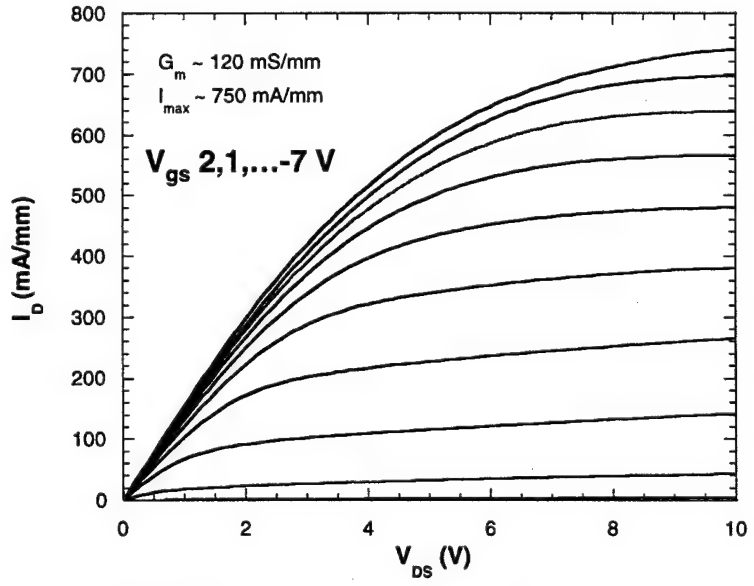

Figure 11. DC I-V characteristics of a 0.25 μm gate length GaN MODFET grown by MBE on sapphire.

Using the fabrication process outlined in the previous section, 0.25 μm gate length GaN MODFET devices were fabricated using this MBE-grown heterostructure material /6/. The MBE-grown GaN MODFET on sapphire, which had a gate width of 100 μm and a source-to-drain spacing of 2 μm exhibited very good DC device characteristics as shown in Figure 11. This device delivered a maximum drain current density (I_{dmax}) of 750 mA/mm which was about 25% lower than that typically exhibited by MOCVD-grown GaN MODFETs /2-3,14,20/. The transconductance (G_m) value measured for this device was 120 mS/mm. The device completely pinched off at a gate bias (V_{gs}) of –7 V.

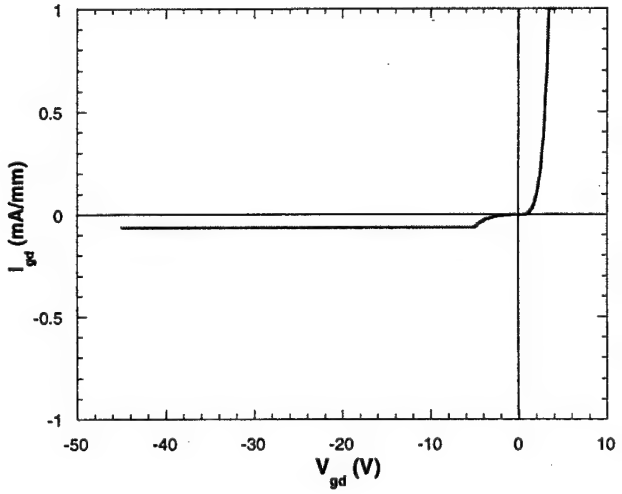

Figure 12. Gate-drain diode characteristics of a 0.25 μm gate length GaN MODFET grown by MBE on sapphire.

The characteristics of the gate-drain diode for this MBE GaN MODFET are shown in Figure 12. The gate to drain spacing in this device was 1.25 μm. The gate Schottky diode had a turn-on voltage (V_{to}) of 1.8V. The reverse bias gate-to-drain breakdown voltage (BV_{gd}) of the device

exceeded 45 V. As discussed in Section II.B., high breakdown voltage, such as that exhibited by this MBE GaN MODFET is a key element in producing high microwave output power.

The small-signal RF performance of this 0.25 μm MBE GaN MODFET was characterized using S-parameter measurements from 0.1 GHz to 50 GHz. Figure 13 shows the small signal frequency performance of this device at a drain bias (V_{ds}) of 10 V and a gate bias (V_{gs}) of –3.5 V. The unity current gain cut-off frequency (f_T) of this device was 28 GHz, and the measured maximum oscillation frequency (f_{max}) was 40 GHz.

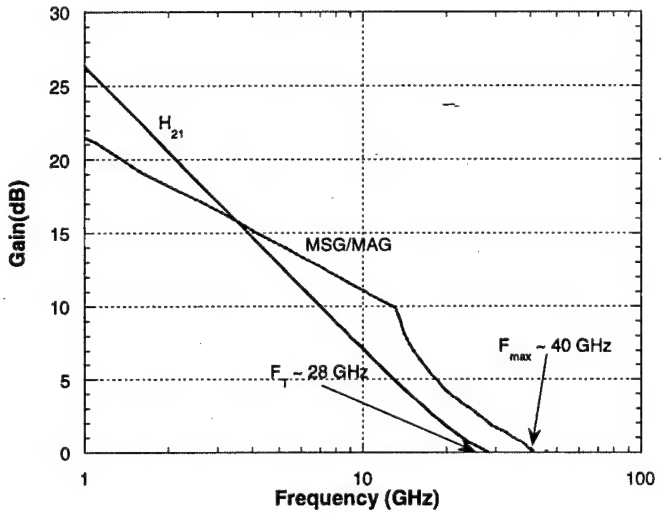

Figure 13. Small signal RF performance of 0.25 X 100 μm GaN MODFET grown by MBE on sapphire.

In order to successfully implement a GaN MODFET microwave power device technology, it is important to be able to scale the devices to gate widths of 1 mm and larger. A key element in this scaling process is the ability to grow GaN MODFET heterostructures with good uniformity. As discussed in Section III.B., GaN MODFET heterostructure material grown by MBE is inherently much more uniform than that grown by MOCVD.

Evidence for the enhanced uniformity of MBE-grown heterostructure material can be found by examining the uniformity of GaN MODFET device characteristics /6/. Specifically, the maximum drain current (I_{dmax}) of a GaN MODFET is one device parameter which is very sensitive to variations in the heterostructure material across the wafer. More importantly, I_{dmax} is one of the key device parameters which defines the microwave output power performance of these devices. As a result, I_{dmax} is an excellent candidate to use as a device parameter to monitor the uniformity of both the GaN MODFET heterostructure material quality and device fabrication.

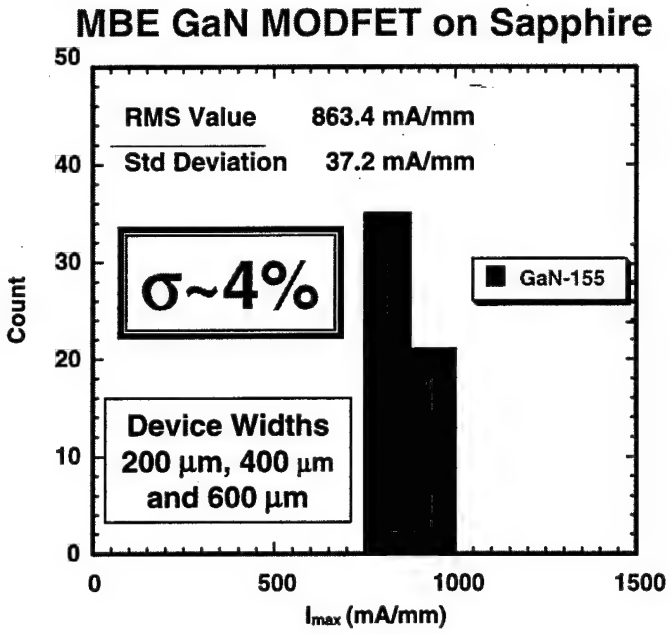

Figure 14. Histogram of maximum drain current density across a quarter of a 2-inch wafer for 0.25 μm GaN MODFETs grown by MBE on sapphire.

GaN MODFET device uniformity was characterized by a comprehensive measurement of the I_{dmax} across a quarter of a 2-inch wafer for devices with gate widths of 200 μm, 400 μm, and 600 μm. The histogram of the normalized maximum drain current density for GaN MODFETs grown

by MBE on sapphire given in Figure 14 shows a very tight distribution of values for I_{dmax}. The RMS value for I_{dmax} for this wafer was about 860 mA/mm, with a standard deviation of approximately 37 mA/mm.

This variation in I_{dmax} of only 4.3% across the wafer is indicative of excellent uniformity in both the MBE-grown GaN MODFET heterostructure materials and the device fabrication process. Indeed, this high level of uniformity is comparable to that found in more mature GaAs-based and InP-based heterostructure device technologies.

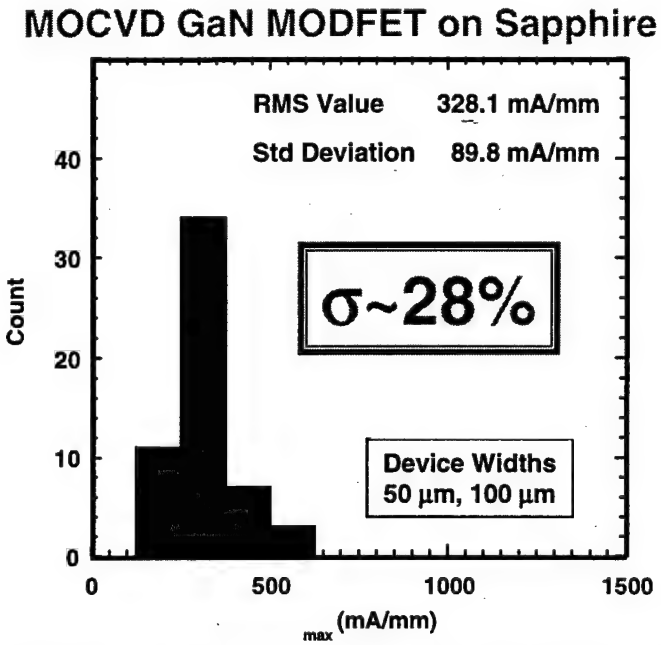

Figure 15. Histogram of maximum drain current density across a quarter of a 2-inch wafer for 0.25 µm GaN MODFETs grown by MOCVD on sapphire.

Shown for comparison in Figure 15 is a similar histogram showing the variation in I_{dmax} across a quarter of 2-inch wafer for GaN MODFETs grown by MOCVD on sapphire. Although the RMS value of 330 mA/mm for I_{dmax} is significantly smaller for this MOCVD-grown wafer, the standard deviation in I_{dmax} is almost three times larger. As a result, the variation in I_{dmax} across

the wafer for these MOCVD-grown GaN MODFETs is 28%. This represents almost a factor of seven increase in the variation in I_{dmax} across a 2-inch wafer compared with that of MBE-grown GaN MODFETs on sapphire.

The excellent uniformity in both the MBE-grown heterostructure material and the fabrication process, as evidenced by the 4% cross-wafer variation in I_{dmax}, provides a strong indication of the scalability of MBE-grown GaN MODFET device technology. In order to examine the scalability of these devices in more detail, it is useful to examine the scalability of I_{dmax} with gate width at relatively high drain biases (i.e., V_{ds} = 10 V) where the drain current saturates in the standard I-V characteristic. Figure 16 shows the transfer characteristics of GaN MODFETs grown by MBE on sapphire with gate widths ranging from 0.2 mm up to 1.0 mm. The characteristic behaviors of the transfer characteristics as a function of gate bias remained the same for all gate widths. For a given gate bias, the drain current of the device scales almost linearly with the gate width. The highest maximum drain current exhibited by the 1.0 mm device was 700 mA.

The transconductance (G_m) peaked at a gate bias of about –4 V for all the different gate width GaN MODFETs with values ranging from 120 mS/mm for the 0.2 mm wide device down to 100 mS/mm for the 1.0 mm wide device. The large 11V voltage swing demonstrated by these devices is a direct result of their high gate-to-drain turn-on voltage (V_{to}) of approximately 2V. These devices also exhibited very high gate-to-drain breakdown voltages in excess of 40V.

In principle, the high level of uniformity observed in I_{dmax} across the wafer should lead to linear scalability of the device parameters as a function of gate widths. In practice, however, the self-generated heat in larger devices can adversely affect device performance. In order to investigate these heating effects, the total maximum drain currents of two different MBE-grown GaN MODFETs on sapphire are shown as a function of the device gate width in Figure 17. It

appears from this curve that the total maximum drain current does scale approximately linearly with the device gate width. In addition, the fact that the total maximum drain currents for the two devices for a given device gate width are almost identical provides strong evidence of the reproducibility both the MBE-growth of GaN MODFET heterostructure material on sapphire and the device fabrication process.

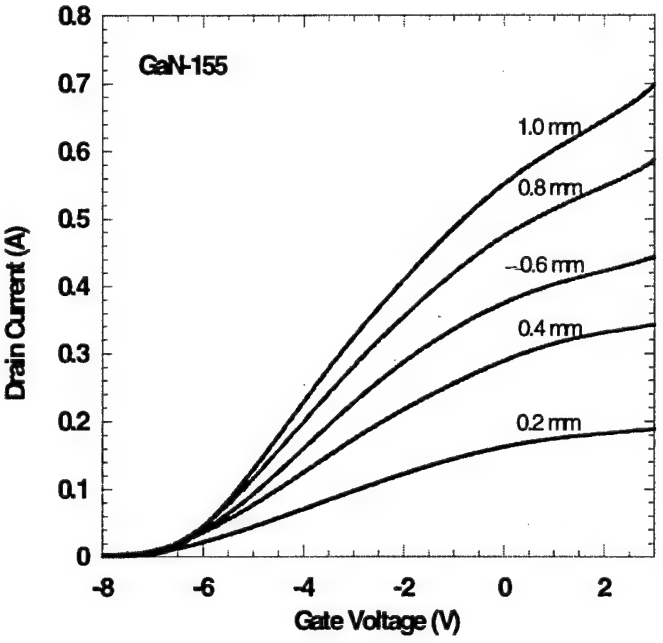

Figure 16. Transfer characteristics of 0.25 μm GaN MODFETs grown by MOCVD on sapphire for gate widths ranging from 0.2 mm up to 1.0 mm.

A closer examination of the maximum drain current density (I_{dmax}) as a function of device gate width makes it clear, however, that the total maximum drain current does not scale linearly with device gate width as originally thought. As shown in the inset in Figure 17, the maximum drain current density drops from a value of 950 mA/mm for the 0.2 mm wide device down to 700 mA/mm for the 1.0 mm wide device. This degradation in the maximum current density (I_{dmax})

with increasing device gate width is a direct result of increased thermal generation for the larger devices. It is important to note, however, that these results were obtained for MBE GaN MODFETs on sapphire that had the thick Au heat-spreaders described in Section III.C, but were not flip-chip mounted to an AlN substrate. The subsequent flip-chip mounting of these devices would undoubtedly reduce the thermal effects in these devices.

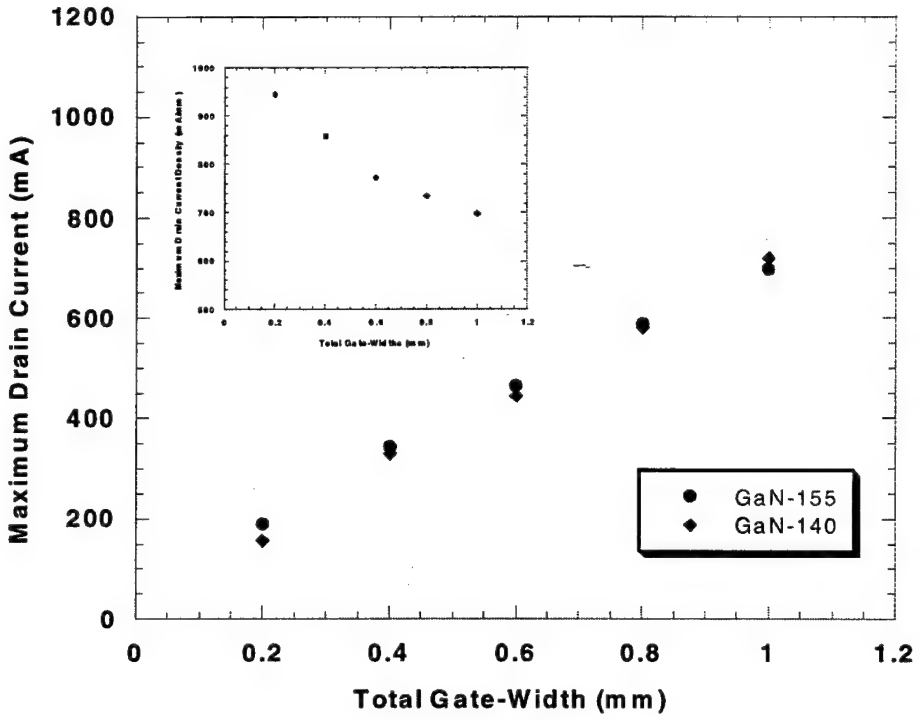

Figure 17. Total maximum drain current and maximum drain current density (inset) as a function of device gate width for 0.25 μm GaN MODFETs grown by MOCVD on sapphire for gate widths ranging from 0.2 mm up to 1.0 mm.

The small-signal RF performance of GaN MODFETs grown by MBE on sapphire were characterized using S-parameter measurements from 0.5 to 26.5 GHz. Figure 18 shows the cut-off frequencies of these devices as a function of the device gate width. The measured unity current gain cut-off frequency (f_T) did not exhibit any strong dependence on device gate width,

varying between 23 GHz and 26 GHz. However, the extrapolated maximum oscillation frequency (f_{max}) peaked at a value of 51GHz for the 0.4 mm wide GaN MODFET and subsequently decreased monotonically with increasing device gate width down to a value of less than 30 GHz for the 1 mm wide device. This roll-off in f_{max} with increasing device gate width was most likely associated with increased parasitic source inductance for the larger GaN MODFET devices.

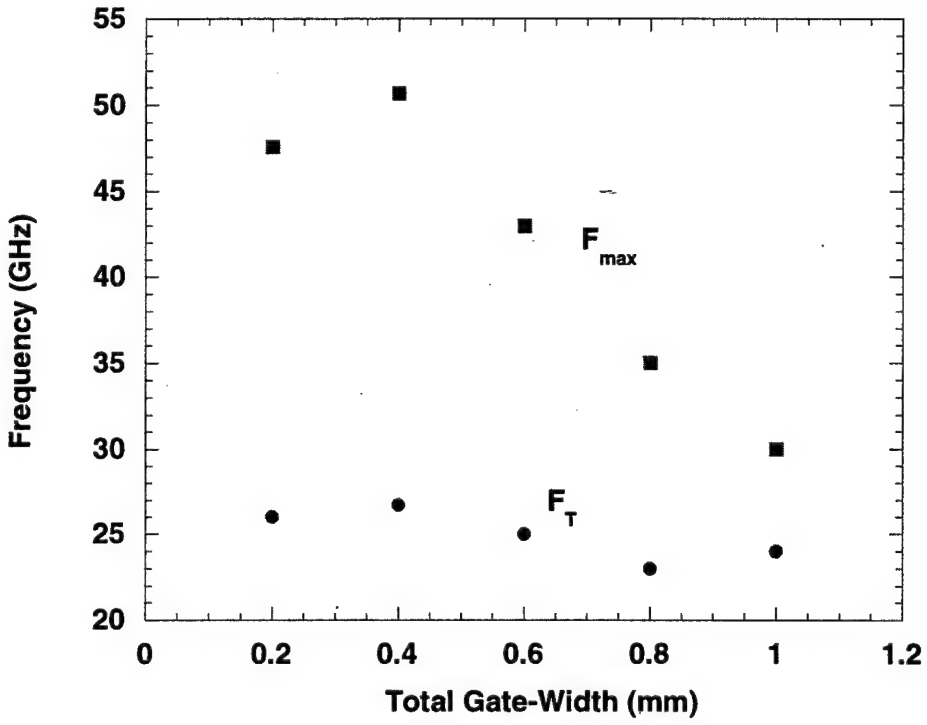

Figure 18. Unity current gain cut-off frequency (f_T) and extrapolated maximum oscillation frequency (f_{max}) of 0.25 μm GaN MODFETs as a function of device gate width.

Another key issue in the development of this GaN MODFET microwave power device technology is the impact of the Au heat-spreader on GaN MODFET device characteristics. As discussed in Section III.C., one major role of the Au heat-spreader is to make the temperature

distribution across a multifinger device much more uniform and prevent hot-spots from forming under certain gate fingers.

A comparison of the DC I-V characteristics of a 0.25 X 200 μm GaN MODFET grown by MBE on sapphire prior to and following the fabrication of the Au heat-spreader is shown in Figure 19. In addition to making the thermal distribution more uniform, the Au heat-spreader has the positive effect of actually transferring the heat away from this device. Evidence for this effect is provided by the 15% to 20% increase in drain current (I_d) demonstrated by these GaN MODFETs following the fabrication of the Au heat-spreader. A much larger enhancement might be expected for devices with gate widths larger than 0.2 mm. Unfortunately, such wider gate width devices cannot be characterized prior to the fabrication of the Au heat-spreader because of the design of HRL's fabrication process.

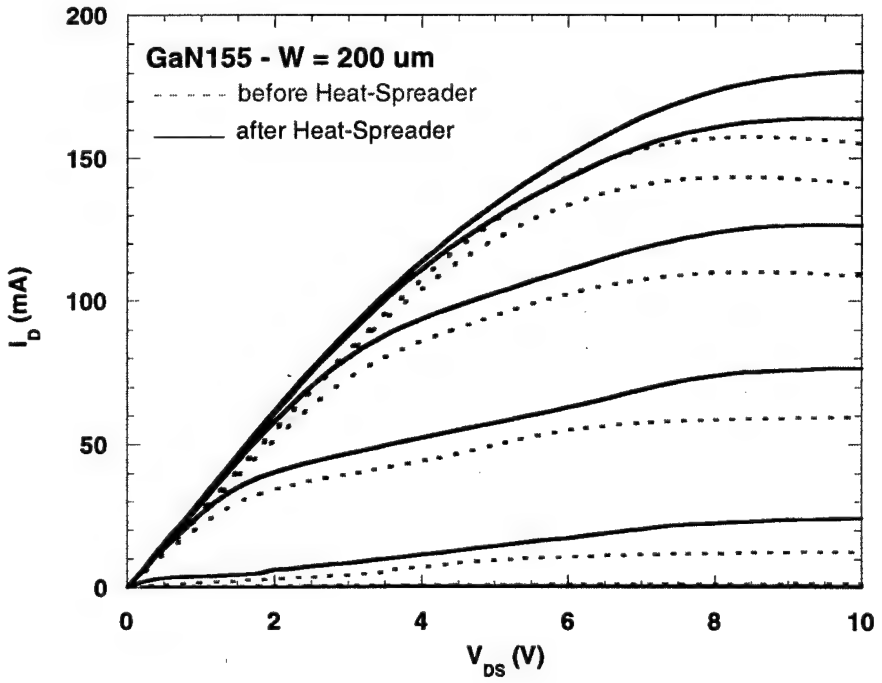

Figure 19. DC I-V characteristics of a 0.25 X 200 μm GaN MODFETs before and after fabrication of Au heat-spreader.

In order to determine the impact of the Au heat-spreader on the small-signal RF performance of these devices, S-parameter measurements were carried out on this same 0.25 X 200 μm MBE GaN MODFETs on sapphire prior to and following the fabrication of the Au heat-spreader. The results of these S-parameter measurements on the GaN MODFET without the heat spreader are shown in Figure 20. The measured unity current gain cut-off frequency (f_T) in this device was 24 GHz, and the extrapolated maximum oscillation frequency (f_{max}) was 57 GHz.

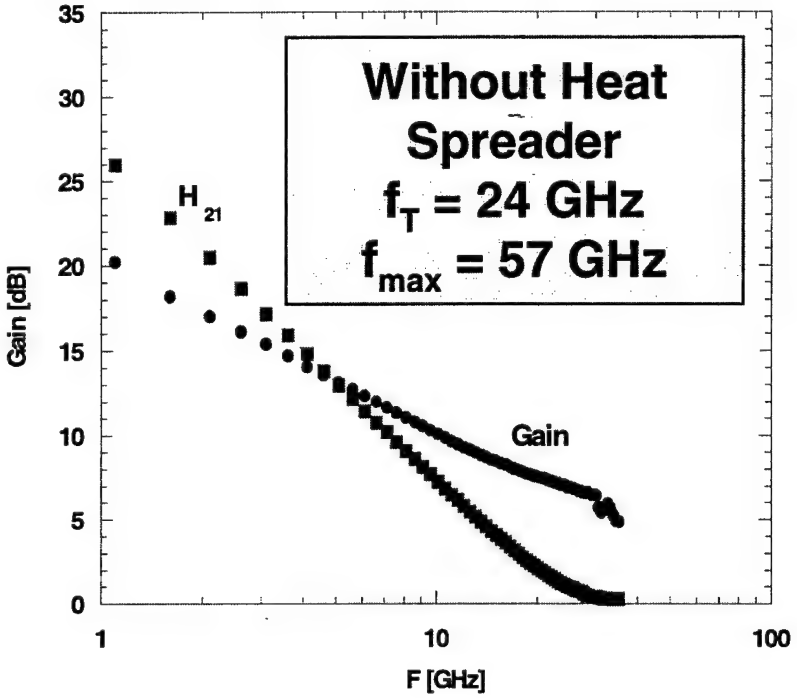

Figure 20. Small signal S-parameter measurements carried out on 0.25 X 200 μm GaN MODFETs prior to fabrication of Au heat-spreader.

Following the fabrication of the Au heat-spreader, the S-parameters for the device were remeasured as shown in Figure 21. The measured values of 26 GHz for the unity current gain cut-off frequency (f_T) and 50 GHz for the extrapolated maximum oscillation frequency (f_{max}) for the GaN MODFET in the presence of the Au heat-spreader are virtually the same as those for the same device without the Au heat-spreader. At least as far as small-signal RF performance of the GaN MODFETs is concerned, therefore, the Au heat-spreader does not have a significant impact on the device. It should be noted, however, that the enhanced thermal management using the Au heat-spreader will likely have a positive effect on the small-signal RF performance of wider gate-width MBE GaN MODFETs on sapphire.

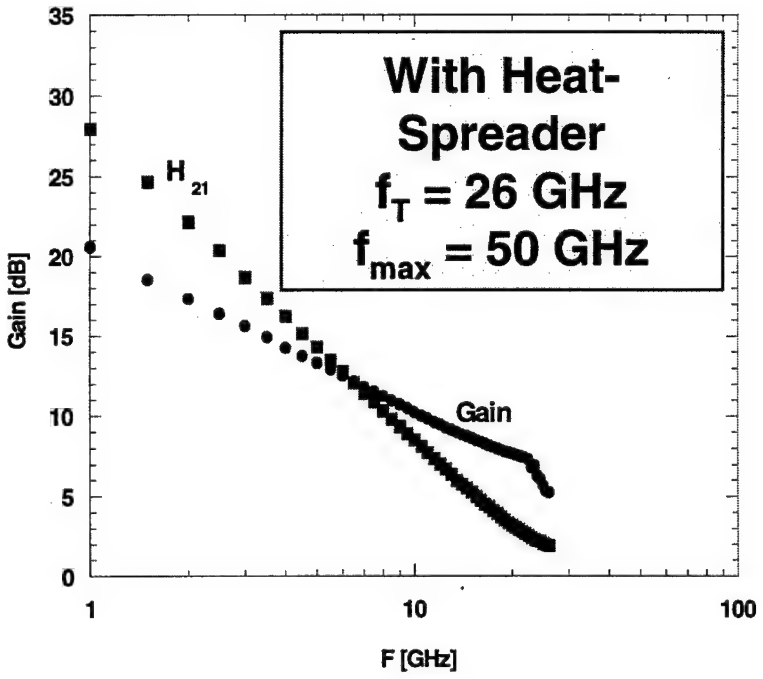

Figure 21. Small signal S-parameter measurements carried out on 0.25 X 200 μm GaN MODFETs following fabrication of Au heat-spreader.

IV.B. Device Performance for MBE GaN MODFETs on GaN Templates

In Section IV.A., the advantages of MBE-grown GaN MODFETs on sapphire over those grown by MOCVD on sapphire in terms of uniformity, and potentially reproducibility, have been quite clearly demonstrated. As discussed in Section III.B., the lower growth temperature inherent in MBE growth of GaN-based materials, and therefore lower differential thermal expansion between the GaN MODFET heterostructure and the sapphire substrate, makes it easier to grow thicker $Al_xGa_{1-x}N$ Schottky layers without cracking of the epilayer material.

As also discussed in Section III.B, however, MBE growth of GaN is much slower than that of MOCVD, thereby making it difficult to grow thicker GaN buffer layers for GaN MODFET devices using MBE. In addition, the initial growth of the thin GaN nucleation layer directly on the sapphire substrate using MOCVD growth has been much more extensively studied, and is presumably more well understood, than it is for MBE.

In order to take full advantage of the strengths of both the MBE and the MOCVD GaN growth techniques, therefore, HRL has developed a hybrid approach involving MBE regrowth of GaN MODFET heterostructures on GaN templates grown on sapphire by MOCVD. A schematic cross-section of a MBE GaN MODFET on GaN templates heterostructure is shown in Figure 22.

This unique MBE GaN MODFET on GaN template approach first uses MOCVD to grow a highly resistive GaN template on sapphire using the standard GaN nucleation layer grown at low temperatures (i.e., typically 600 °C), and a thicker GaN buffer layer grown at higher temperatures (i.e., between 1000 °C and 1100 °C). This MOCVD-grown GaN template on a sapphire substrate is then transferred to the MBE growth system. Here, an additional GaN buffer and channel layer is grown by MBE on top of the GaN template. Continuing without interruption, MBE is then

used to grow the $Al_xGa_{1-x}N$ Schottky layer at an Al mole fraction of x = 0.3. As was the case for the GaN MODFETs grown directly on sapphire by MBE, this Schottky layer consisted of a 30 Å unintentionally doped (UID) $Al_xGa_{1-x}N$ spacer layer, a 50 Å $Al_xGa_{1-x}N$ layer doped n-type with Si at 2 X 10^{19} cm^{-3}, and a 250 Å unintentionally doped (UID) $Al_xGa_{1-x}N$ cap layer. These MBE GaN MODFET heterostructures on GaN templates typically exhibited an electron mobility of approximately 1000 cm^2/V-S at a sheet carrier concentration in the range of 1 – 2 X 10^{13} cm^{-2}.

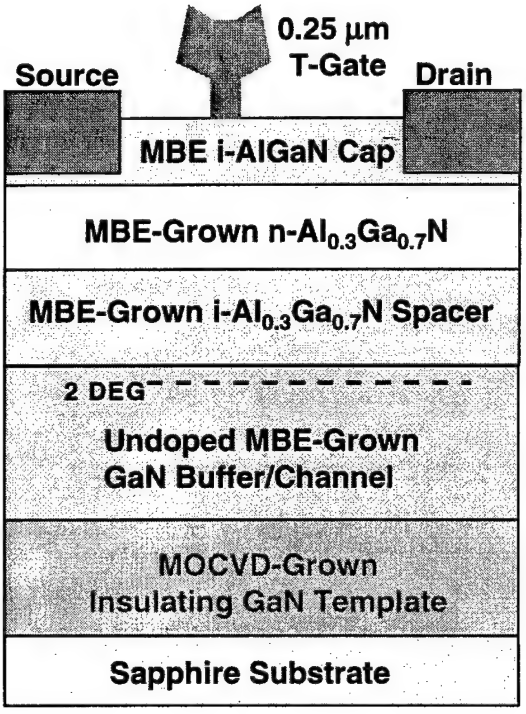

Figure 22. $Al_xGa_{1-x}N$/GaN MODFET device heterostructure grown using MBE on a MOCVD-grown GaN template on sapphire.

The DC I-V characteristics of a 0.25 X 100 µm MBE GaN MODFET on a GaN template is shown in Figure 23. This device exhibits a maximum drain current density (I_{dmax}) of 950 mA/mm

and a transconductance (G_m) of 200 mS/mm. The gate-to-drain breakdown voltage (BV_{gd}) for this device is over 60V. These DC device characteristics represent a substantial improvement over those demonstrated by GaN MODFETs grown directly on sapphire by MBE as presented in Section IV.A. In fact, the DC device characteristics of these MBE GaN MODFET on GaN template devices are actually comparable to the better results reported for GaN MODFETs grown by MOCVD on sapphire /2-4,14,20,31/.

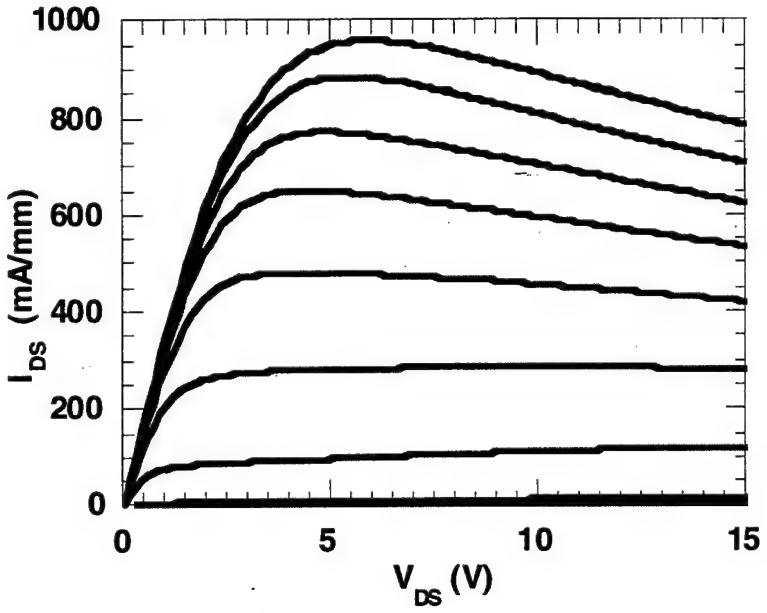

Figure 23. DC I-V characteristics of a 0.25 μm MBE-grown GaN MODFET on a MOCVD-grown GaN template.

As might be expected from the fact that MBE is used to grow the actual active device portion of the GaN MODFET heterostructure for these devices, the uniformity of these DC device characteristics is almost identical to those for GaN MODFETs grown directly on sapphire by MBE. Figure 24 shows a histogram of the maximum drain current (I_{dmax}) for 0.25 μm MBE GaN

MODFETs on GaN templates for 200 μm, 400 μm, and 600 μm wide devices across a quarter of a 2-inch wafer. The RMS value for I_{dmax} for this wafer was about 850 mA/mm, with a standard deviation of approximately 35 mA/mm.

This variation in I_{dmax} across the wafer of only 4.1% is indicative of the excellent uniformity in both the MBE-grown GaN MODFET on GaN template heterostructure materials and the device fabrication process. In fact, this variation is virtually identical to the 4.3% variation in I_{dmax} measured for GaN MODFETs grown directly on sapphire by MBE and is several times smaller than the 28% variation for MOCVD-grown GaN MODFETs discussed in Section IV.A.

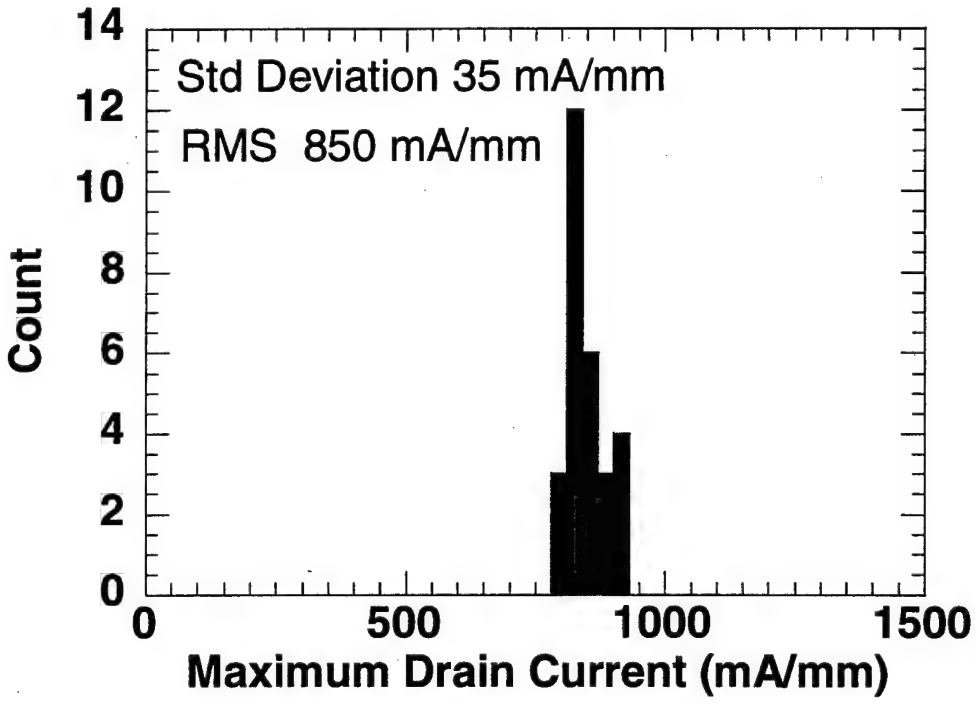

Figure 24. Histogram of maximum drain current density across a quarter of a 2-inch wafer for 0.25 μm MBE-grown GaN MODFETs on a MOCVD-grown GaN template.

The excellent uniformity in these MBE GaN MODFETs on GaN templates should lead to scalability of these devices with gate width. Figure 25 shows the total maximum drain current of two different 0.25 μm MBE GaN MODFET on GaN template devices with gate widths from 0.2 mm all the way up to 2 mm. The total maximum current scales very linearly up to a gate width of 1 mm. The maximum current density (I_{dmax}) in this range is constant at a value of 800mA/mm. As the device width is increased further to 2mm, the maximum current density (I_{dmax}) drops by 20%. As was the case for GaN MODFETs grown on directly on sapphire by MBE, this decrease in maximum current density is associated with the increased thermal generation for the larger devices. In contrast to devices grown directly on sapphire by MBE, however, this device heating effect does not appear to affect the maximum current density in MBE GaN MODFET on GaN template devices until the gate width exceeds 1 mm.

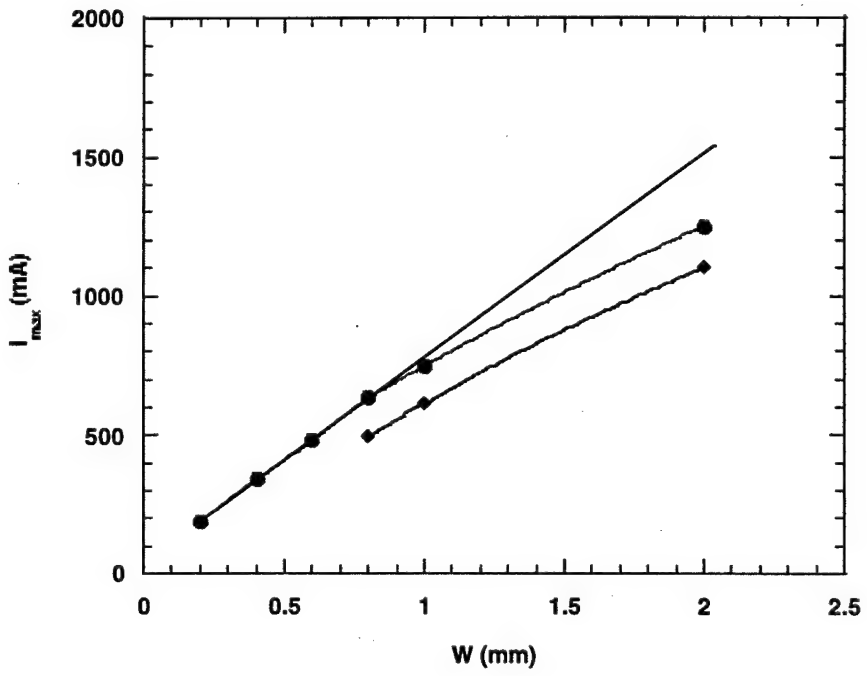

Figure 25. Total maximum drain current as a function of device gate width for 0.25 μm MBE-grown GaN MODFETs on a MOCVD-grown GaN template.

These MBE GaN MODFET on template devices also exhibit very good small signal RF performance. Figure 26 shows the S-parameter measurements on a 0.25 μm device. The unity current gain cut-off frequency (f_T) for this device is 35 GHz, which is substantially higher than the 28 GHz value measured for the equivalent GaN MODFET device grown directly on sapphire by MBE. The extrapolated maximum oscillation frequency (f_{max}) is 50 GHz for this device, which is also somewhat higher than the 40 GHz result obtained for the equivalent device grown directly on sapphire by MBE.

Overall, it appears that the DC and small signal RF performance of MBE GaN MODFETs on GaN templates is significantly better than that of equivalent GaN MODFET devices grown directly on sapphire by MBE. This is undoubtedly due to improved GaN MODFET heterostructure material quality grown by MBE on the MOCVD-grown GaN template material.

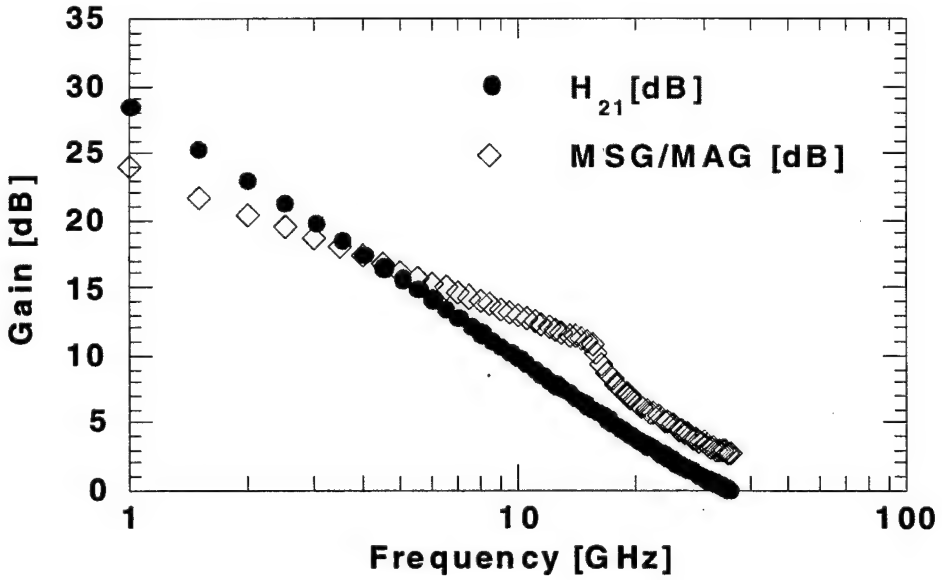

Figure 26. Small signal S-parameter measurements carried out on 0.25 X 200 μm GaN MODFETs grown by MBE on GaN Templates.

IV.C. Microwave Power Performance of MBE GaN MODFETs

Working in conjunction with the University of Michigan, HRL investigated the microwave power performance of GaN MODFETs grown on sapphire by MBE /7/. An on-wafer active load-pull measurement system was used to obtain the P_{out}-P_{in} characteristics of these devices at a frequency of 8 GHz. Both source and load tuners were initially positioned to obtain best matching, and therefore maximum gain, at an input power level corresponding to 1dB gain compression and load terminations corresponding to small signal matching conditions. The source and load tuners were then adjusted to improve matching and maximize the gain.

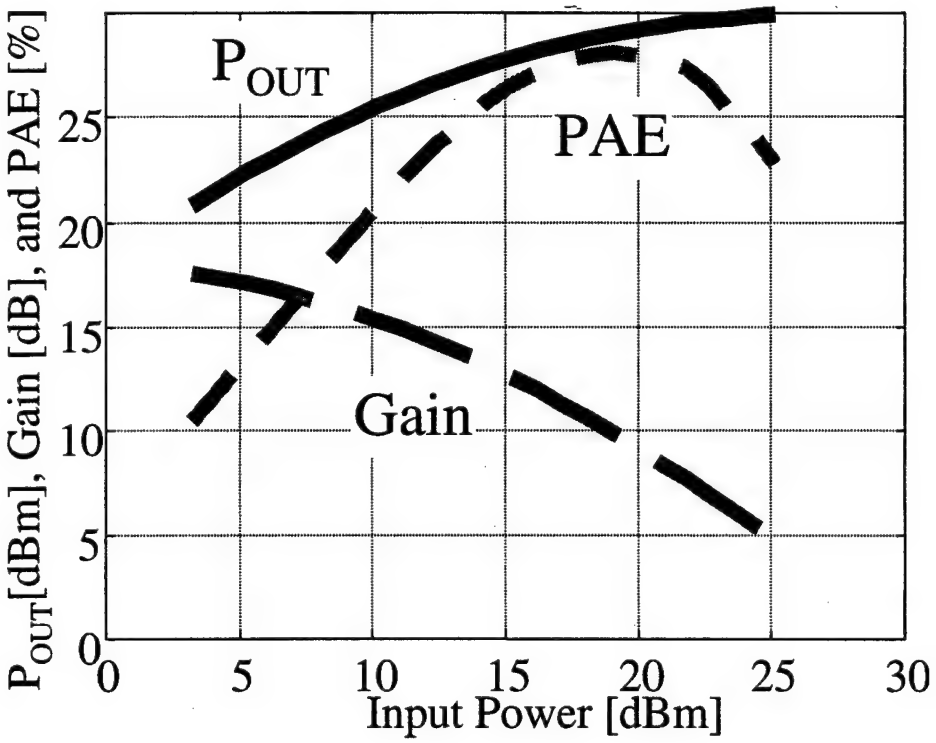

Figure 27. Power performance of a 0.25 μm X 1mm GaN MODFET grown by MBE on sapphire.

The power performance of a 0.25 μm X 1mm MBE-grown GaN MODFET on sapphire is shown in Figure 27. Source and load tuners were optimized for a maximum small signal linear gain of 17.6 dB at 8 GHz. The peak output power ($P_{out-max}$) for this 1 mm wide device was 29.9 dBm, corresponding to an output power (P_{out}) of 1W and an output power density (PD_{out}) of 1W/mm. Under the conditions for peak output power, the power added efficiency (PAE) of the device was 23%, and the associated gain was 4dB. At an input power of 17 dBm, the device exhibited maximum PAE of 28% with an associated gain of 10dB.

An even higher output power density of 1.3W/mm was obtained for a 0.25 μm X 0.6 mm MBE-grown GaN MODFETs on sapphire. This 0.6 mm wide device also showed a somewhat higher linear gain of 18.2 dB and PAE of 29.5%

Constant output power (P_{out}) and constant power added efficiency (PAE) contours of MBE GaN MODFETs on sapphire were also evaluated using the active load-pull system at a frequency of 8 GHz. These contours provide important information regarding the loading conditions for maximum output power and efficiency as necessary for circuit design. Both the constant P_{out} and the constant PAE contours of an 0.25 μm X 0.8 mm MBE GaN MODFET under high input power conditions (i.e., P_{in} = 22 dBm) are shown in Figure 28.

The contours remain circular up to power levels corresponding to severe gain compression (i.e., 10dB). More importantly, it can be seen from Figure 28 that the position for optimal load for maximum output power (P_{out}) of 28 dBm is very close on the Smith Chart to the position for optimal load for maximum power added efficiency (PAE) of 32%. This suggests that power amplifiers can be designed using this device which will not require a significant tradeoff between output power and power-added efficiency.

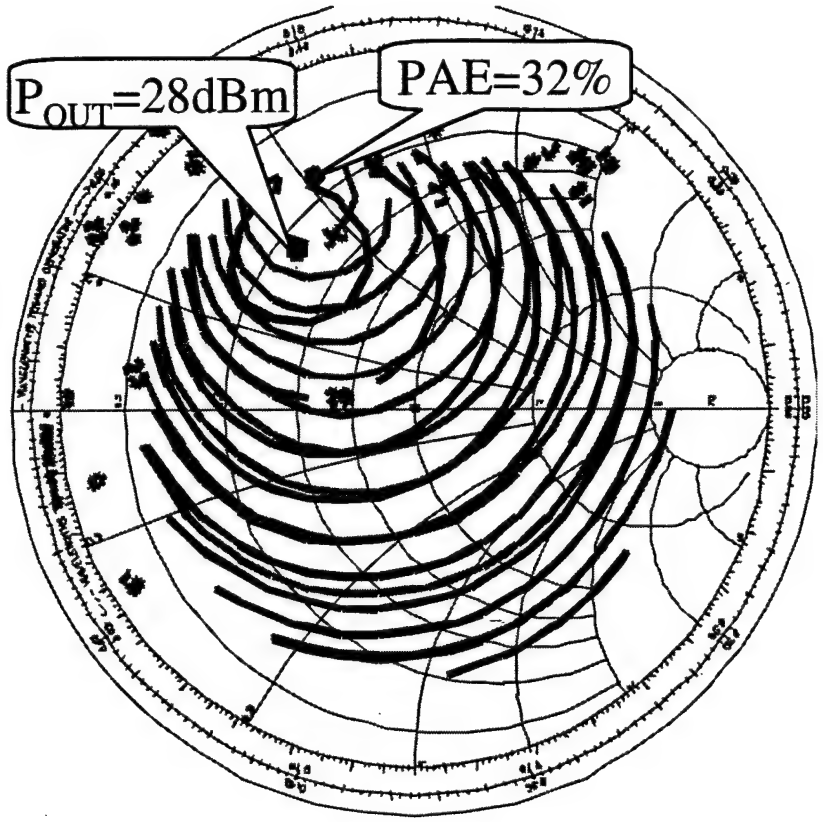

Figure 28. Constant output power (P_{out}) and constant power added efficiency (PAE) contours for a 0.25 μm X 0.8 mm GaN MODFET grown by MBE on sapphire.

V. MOCVD-Grown GaN MODFET Microwave Power Performance

V.A. Low Al Mole Fraction MOCVD GaN MODFETs

GaN MODFETs with 0.25 μm gates were also fabricated under this program by the HRL/UCSB team using MOCVD GaN MODFET heterostructure material grown on sapphire by MOCVD at UCSB /2-5/. The heterostructure for these devices consisted of a 200 Å GaN nucleation layer directly on the c-plane sapphire substrate, followed by a 2 μm thick insulating GaN buffer layer and an $Al_xGa_{1-x}N$ Schottky layer with a relatively low Al mole fraction of x = 0.175. This Schottky layer was comprised of a 30 Å unintentionally doped (UID) $Al_xGa_{1-x}N$ spacer layer, a 120 Å $Al_xGa_{1-x}N$ charge donor layer doped with Si at 6 X 10^{18} cm^{-3}, and a 50 Å UID $Al_xGa_{1-x}N$ cap layer.

These 0.25 μm $Al_xGa_{1-x}N$/GaN MODFET (x = 0.175) devices grown by MOCVD on sapphire exhibited very good DC and small-signal RF performance. The maximum drain current for these 0.25 μm MOCVD-grown GaN MODFET on sapphire devices was 800 mA/mm. The devices also exhibited very high transconductance (G_m) values of 240 mS/mm, and a reverse bias gate-to-drain breakdown voltage (BV_{gd}) of 80 V per micron of gate-to-drain spacing.

Figure 29 shows the small-signal S-parameter measurements on 0.25 X 25 μm MOCVD-GaN MODFET on sapphire devices. The unity current gain cut-off frequency (f_T) of this device was 50 GHz, and the extrapolated maximum oscillation frequency (f_{max}) was 92 GHz. These results are significantly higher than the values obtained for MBE GaN MODFETs on sapphire as discussed in Section IV. Indeed, these are among some of the very highest combined values for f_T and f_{max} ever demonstrated by any GaN MODFET device /2/.

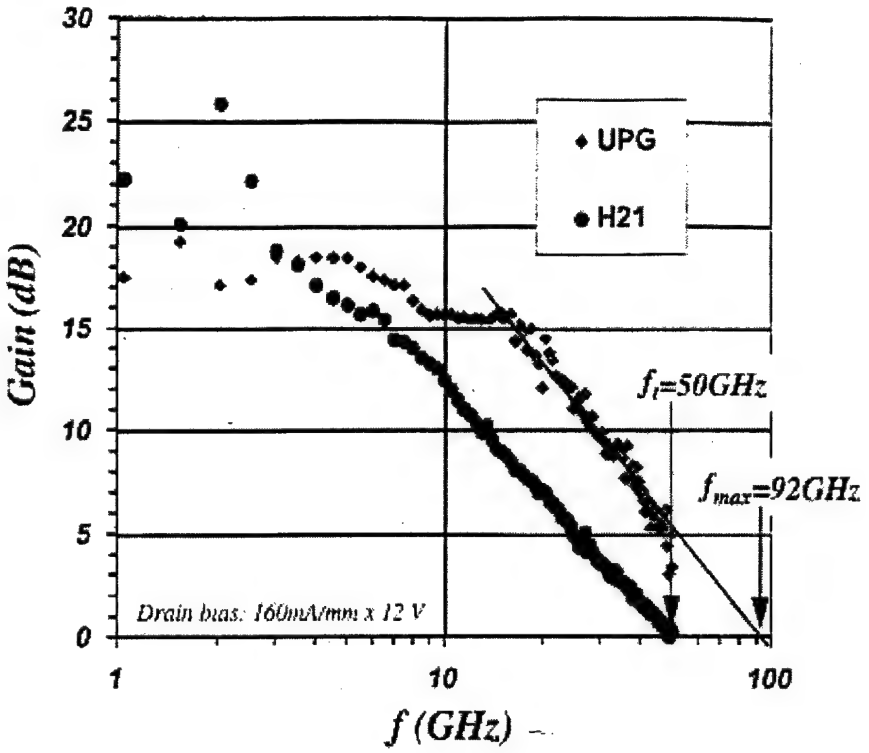

Figure 29. Small signal RF performance of a 0.25 X 25 μm $Al_xGa_{1-x}N$/GaN MODFET (x = 0.175) grown by MOCVD on sapphire.

The power performance of these 0.25 μm MOCVD GaN MODFET on sapphire devices was characterized at 10 GHz using an on-wafer active load-pull measurement system /2/. The measured P_{out}-P_{in} characteristics of a 0.25 X 100 μm device is shown in Figure 30. The peak output power (P_{out-pk}) for this device was 22.3 dBm, corresponding to an output power density (PD_{out}) of 1.70 W/mm. The large signal and small-signal linear gain were 6.3 dB and 11.4 dB respectively. This device exhibited a power-added efficiency (PAE) of 23% under the conditions for peak output power .

The output power (P_{out}) of this MOCVD GaN MODFET on sapphire device was not large (i.e., 170 mW) owing to the relatively small 100 μm gate width of the device. However the output power density (PD_{out}) of 1.7 W/mm is substantially higher than the highest value of 1.3

W/mm obtained for the MBE GaN MODFET on sapphire presented in Section IV.C. Both the MOCVD-grown and the MBE- grown GaN MODFET on sapphire devices exhibited power-added-efficiencies (PAE) of 23%.

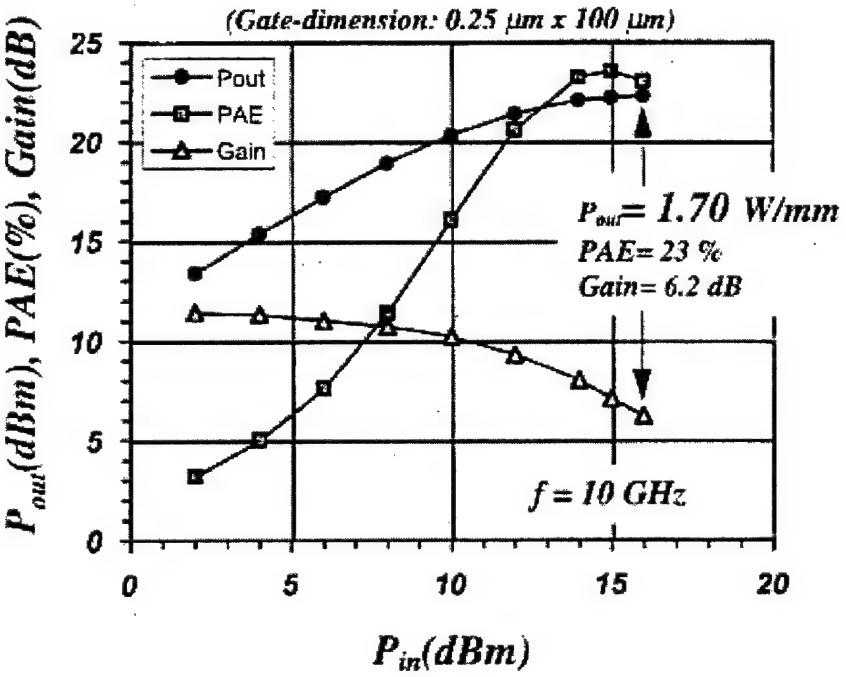

Figure 30. Microwave power performance of a 0.25 X 100 μm $Al_xGa_{1-x}N$/GaN MODFET (x = 0.175) grown by MOCVD on sapphire.

IV.B. High Al Mole Fraction MOCVD GaN MODFETs on Sapphire

Further improvement in the output power density (PD_{out}) of an MOCVD-grown GaN MODFET on sapphire was achieved by increasing the Al mole fraction of the $Al_xGa_{1-x}N$ Schottky layer to x = 0.5 /2-4, 14/. Figure 31 illustrates the improved power performance of an 0.25 μm X 0.5 mm MOCVD GaN MODFET on sapphire at a frequency of 8 GHz. From these The P_{out}-P_{in} characteristics, it can be seen that the peak output power (P_{out-pk}) for this device was

30 dBm. The resulting power density (PD_{out}) of this 1 Watt device was 2 W/mm. Under conditions for peak output power, the large signal of the device was 4dB and the power-added efficiency (PAE) was 23%.

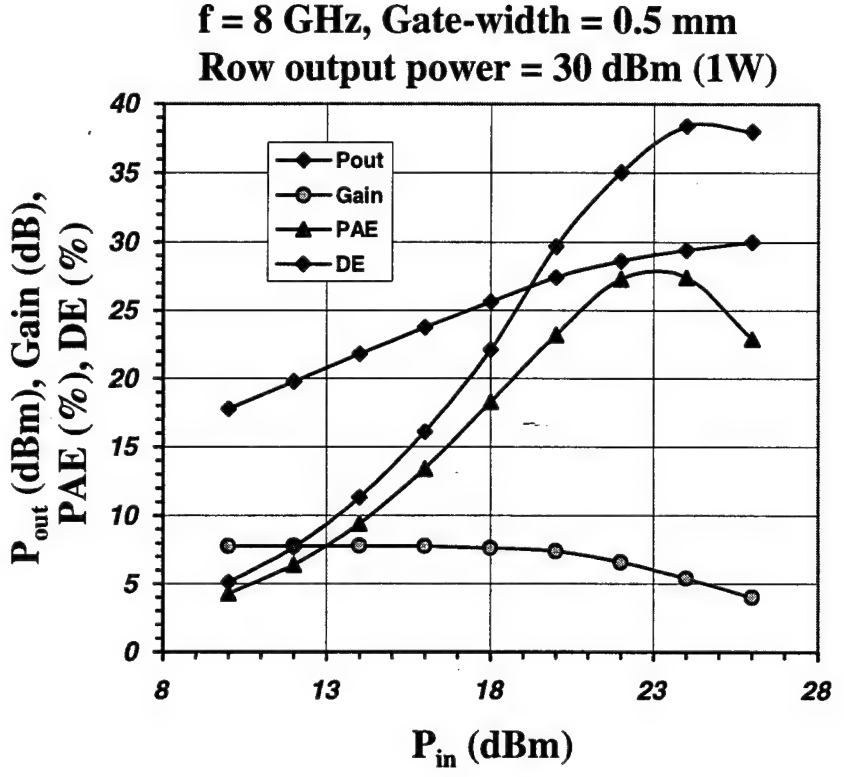

Figure 31. Microwave power performance of a 0.25 μm X 0.5 mm $Al_xGa_{1-x}N$/GaN MODFET (x = 0.5) grown by MOCVD on sapphire.

Because no flip-chip thermal management was attempted for this device during these power measurements, self-heating effects no doubt had an impact on the microwave power performance of this device. Indeed, reducing the gate width of this high Al mole fraction (i.e.,x = 0.5) 0.25 μm MOCVD GaN MODFET on sapphire resulted in a significant increase in the microwave output power density (PD_{out}). Figure 32 shows the peak output power (P_{out-pk}) and the output power

density (PD_{out}) as a function of gate width for this high Al mole fraction MOCVD GaN MODFET on sapphire. As the gate width was reduced from 0.5 mm down to 0.1 mm, the microwave output power density increased dramatically from 2 W/mm up to 3.3 W/mm. This dramatic change in PD_{out} could be due to self-heating effects which would be expected to have an increasingly negative impact on the microwave power performance of the device as its gate width increases. In addition, this 40% decrease in $PD_{out,}$, which ultimately limits the total power of the device, may also be indicative of some significant nonuniformity in the heterostructure material or the device processing for these MOCVD GaN MODFETs.

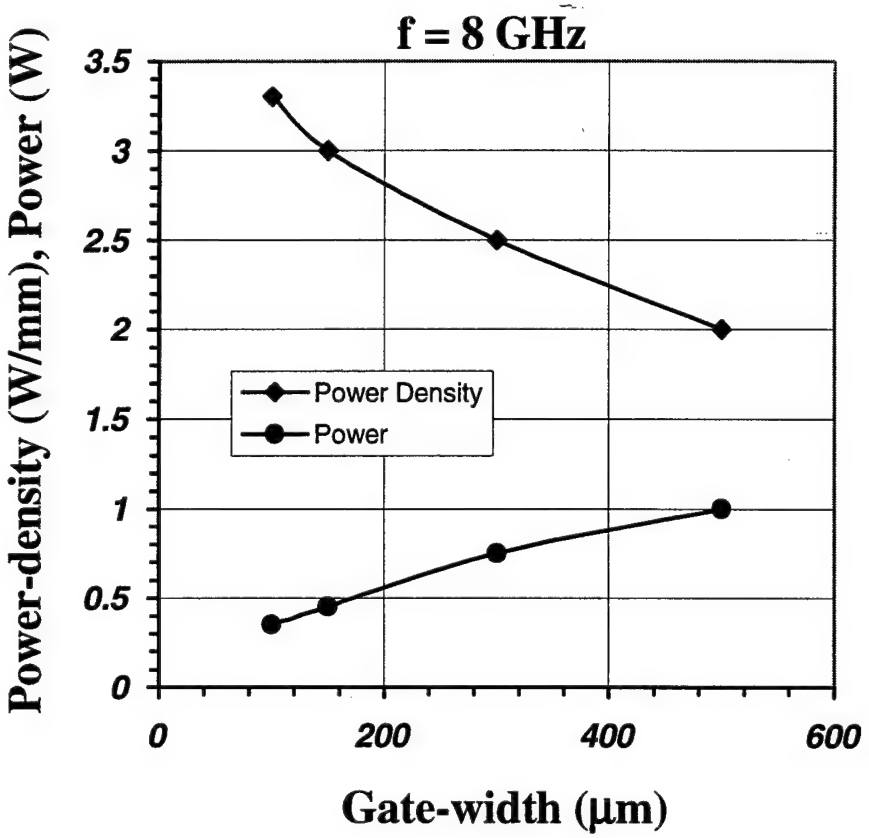

Figure 32. CW microwave output power density (PD_{out}) and total power (P_{out}) at 8 GHz as a function of gate periphery for a 0.25 μm GaN MODFET grown by MOCVD on sapphire.

The microwave power performance of MOCVD GaN MODFETs on sapphire have also been measured at a K-Band frequency of 18 GHz /3/. The P_{out}-P_{in} characteristics of a 0.25 X 76 μm MOCVD GaN MODFET on sapphire is shown in Figure 33. This device exhibited excellent DC characteristics with a maximum drain current (I_{dmax}) of 1.1 A/mm and a gate-to-drain breakdown voltage (BV_{gd}) of over 70 V. The small signal RF performance of this device from S-parameter measurements was also very good. The unity current-gain cutoff frequency (f_T) of this 0.25 μm MOCVD GaN MODFET was 52 GHz, and its maximum frequency of oscillation (f_{max}) was 82 GHz.

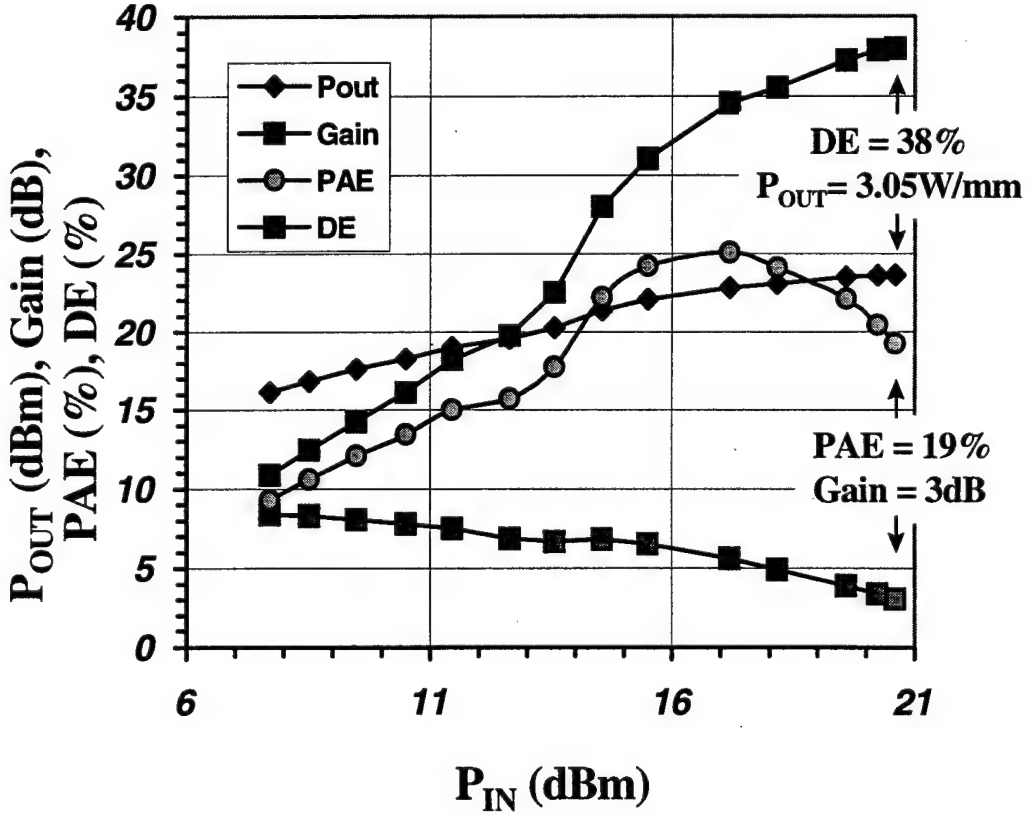

Figure 33. Microwave power performance of 0.25 X 76 μm MOCVD GaN MODFET on sapphire measured at 18 GHz.

As shown in Figure 33, the peak output power ($P_{out\text{-}pk}$) of this 0.25 X 76 μm MBE GaN MODFET was 23.65 dBm at a frequency of 18 GHz. This corresponds to a microwave output power density (PD_{out}) of 3.05 W/mm. Under the conditions for peak power, the large signal gain for this device was 3.1 dB, and the power added efficiency (PAE) was 19.2%.

This microwave output power density of 3.05 W/mm represents the highest value every reported for any device/materials FET technology at this frequency of 18 GHz. Indeed, this value for PD_{out} is well over three times larger than the power densities generally achieved using GaAs-based FET technologies.

VI. Conclusions

Under this program, the HRL/UCSB team has demonstrated GaN MODFET devices with microwave power densities at X-Band and K-Band frequencies that are several times larger than conventional solid state microwave power devices such as GaAs-based PHEMTs. The results of this program form the basic foundation for the development of a GaN MODFET technology capable of revolutionizing the field of microwave power electronics /1/.

The HRL/UCSB team has developed the essential elements for such a GaN MODFET technology including material growth, device fabrication, thermal management, and device characterization. Under this program, excellent quality GaN MODFET heterostructure device material has been successfully grown using both Molecular Beam Epitaxy (MBE) and Metal-Organic Chemical Vapor Deposition (MOCVD) material growth techniques. A 0.25 μm gate length GaN MODFET fabrication process has been developed which is capable of producing microwave power devices operating at frequencies from X-Band up to K-Band frequencies. Integrated into this fabrication process is a unique heat-spreader/flip-chip thermal management approach which addresses the critical issues associated with self-generated heating which can ultimately limit the performance of GaN MODFET microwave power devices.

Using GaN MODFET heterostructure device material grown by MBE directly on sapphire or on GaN template material (i.e., GaN grown on sapphire by MOCVD), the HRL/UCSB team has demonstrated GaN MODFET devices with excellent DC and small signal RF characteristics. These 0.25 μm MBE GaN MODFETs exhibit excellent device uniformity (i.e., variation ~ 4 % across a 2-in. wafer) which is comparable to more conventional and well-established GaAs- and InP-based FET technologies. Under this program, the HRL/UCSB team has also demonstrated

the first MBE GaN MODFET capable of producing 1 Watt of microwave output power at a frequency of 8 GHz. These MBE GaN MODFETs exhibited microwave power densities of up to 1.3 W/mm at this frequency.

The HRL/UCSB team has also developed a 0.25 μm MOCVD-grown GaN MODFETs with extremely high power densities at X-Band and K-band frequencies under this program. MOCVD GaN MODFETs have been demonstrated with microwave output power densities of 3.3 W/mm at a frequency of 8 GHz. MOCVD GaN MODFET devices capable of producing up to 1 Watt of microwave output power at 8 GHz have been demonstrated. In addition, MOCVD GaN MODFET devices have been developed which exhibit microwave output power densities of 3.05 W/mm at a frequency of 18 GHz.

All of these results point to the successful development of a very high performance GaN MODFET microwave power device technology under this program. As a result, this program has provided the basic foundation for the development of a high performance GaN MODFET technology that will indeed revolutionize the field of microwave power electronics.

VII. Acknowledgements

This work was possible with the efforts of many individuals at HRL Laboratories and the University of California at Santa Barbara (UCSB). The author would also like to recognize close collaboration with researchers at the University of Michigan. The authors would also to thank the continued support and enthusiasm of Elliot Brown, Gerald Witt, and Edgar Martinez.

VIII. References

[1] D.E. Grider, N.X. Nguyen, and C. Nguyen, "GaN MODFET Microwave Power Technology for Future Generation Radar and Communication Systems", submitted *to Solid State Electronics.*

[2] Y.F. Wu, B.P. Keller, S.Keller, N.X. Nguyen, M. Le, C. Nguyen, T.J. Jenkins, L.T. Kehias, S.P. Denbaars, and U.K. Mishra, "Short Channel AlGaN/GaN MODFETs with 50 GHz f_T and 1.7 W/mm Output Power at 10 GHz", *IEEE Electron Device Letters*, vol. 18, pp. 438-440, 1997.

[3] Y.F. Wu, B.P. Keller, P. Fini, J. Pusl, M. Le, N.S. Nguyen, C. Nguyen, D. Widman, S. Keller, s.P. Denbaars, and U.K. Mishra, "Short-Channel $Al_{0.5}Ga_{0.5}N$,/GaN MODFETs with Power Density > 3 W/mm at 18 GHz," *Electronics Letters*, vol. 33, pp. 1742-1743, 1997.

[4] N.X. Nguyen, B.P. Keller, S. Keller, Y.F. Wu, M. Le, C. Nguyen, S.P. Denbaars, U.K. Mishra, and D. Grider, "GaN/AlGaN MODFET with 80 GHz f_{max} and > 100 V Gate-Drain Breakdown Voltage," *Electronics Letters*, vol. 33, pp. 334-335.

[5] N.X. Nguyen, C. Nguyen, and D.E. Grider, "Device Characteristics of Scaled AlGaN/GaN MODFETs," *Electronics Letters*, vol. 34, pp. 811-812, 1998.

[6] C. Nguyen, N.X. Nguyen, M. Le, and D.E. Grider, "High Performance GaN/AlGaN MODFETs Grown by RF-Assisted MBE," *Electronics Letters*, vol. 34, pp. 309-310, 1998.

[7] E. Alekseev, D. Pavlidis, N.S. Nguyen, C. Nguyen, and D.E. Grider, "Large-Signal Characteristics of AlGaN/GaN Power MODFETs," *1999 IEEE MTT-S Digest*, pp. 533-536, 1999.

[8] G. Sullivan, E. Gertner, R. Pittman, M. Chen, R. Pierson, A. Higgens, "AlGaN Microwave Power HFETs on Insulating SiC Substrates," *1999 Materials Research Society Symposium Proceedings*, vol. 572, pp. 471-479, 1999.

[9] S.T. Allen, S.T. Sheppard, W.L. Pribble, R.A. Sadler, T.S. Alcorn, Z. Ring, and J.W. Palmour, "Recent Progress in SiC Microwave MESFETs", *1999 Materials Research Society Symposium Proceedings*, vol. 572, pp. 15-22, 1999.

[10] S.T. Sheppard, K. Doverspike, W.L. Pribble, S.T. Allen, J.W. Palmour, L.T. Kehias, and T.J. Jenkins, "High Power GaN/AlGaN HEMTs on Silicon Carbide, *1998 Device Research Conference Abstracts*, Charlottesville, VA, 1998.

[11] G.J. Sullivan, M.Y. Chen, J.A. Higgins, J.W. Yang, Q. Chen, R.O. Pierson, and B.T. McDermott, "High Power RF Operation of AlGaN/GaN HEMTs Grown on Insulating Silicon Carbide Substrates," *Electronics Letters*, vol. 19, pp. 198-200, 1998.

[12] G.J. Sullivan, J.A. Higgins, M.Y. Chen, J.W. Yang, Q. Chen, R.L. Pierson, and B.T. McDermott, "High Power RF Operation of AlGaN/GaN HEMTs Grown On Insulating Silicon Carbide Substrates," *Electronics Letters*, vol. 34, pp. 922-924, 1998.

[13] Q. Chen, J.W. Yang, R. Gaska, M. A. Khan, M.S. Shur, G.J. Sullivan, A.L. Sailor, J.A. Higgins, A.T. Ping, and I. Adesida, "High-Power Microwave 0.25 μm Gate Doped-Channel GaN/AlGaN Heterostructure Field Effect Transistor," *IEEE Electron Device Letters*, Vol. 19, pp. 44-46, 1998.

[14] Y.F. Wu, B.P. Keller, P. Fini, S. Keller, T.J. Jenkins, L.T. Kehias, S.P. Denbaars, and U.K. Mishra, "High Al Content AlGaN/GaN MODFETs for Ultrahigh Performance," *IEEE Electron Device Letters*, vol 19, pp. 50-53, 1998.

[15] E.T. Yu, G.J. Sullivan, P.M. Asbeck, C.D. Wang, D. Qiao, and S.S. Lau, "Measurement of Piezoelectrically Induced Charge in GaN/AlGaN Heterostructure Field Effect Transistors," *Applied Physics Letters*, vol. 71, pp. 2794-2796, 1997.

[16] R. Gaska, Q. Chen, J. Yang, A. Osinsky, M. A. Khan, and M. S. Shur, "High-Temperature Performance of AlGaN/GaN HFET's on SiC Substrates," *IEEE Electron Device Letters*, vol. 18, pp. 492-494, 1997.

[17] Q. Chen, J. W. Yang, M. A. Khan, A. T. Ping, and I. Adesida, "High Transconductance AlGaN/GaN Heterostructure Field Effect Transistors on SiC Substrates," *Electronics Letters*, vol. 33, pp. 1413-1415, 1997.

[18] R. Gaska, Q. Chen, J. Yang, A. M. Khan, M. S. Shur, A. Ping, and I. Adesida, "AlGaN-GaN Heterostructure FETs with Offset Gate Design," *Electronics Letters*, vol. 33, pp. 1255-1257, 1997.

[19] O. Aktas, Z.F. Fan, A. Botchkarev, S.N. Mohammad, M. Roth, T. Jenkins, L. Kehias, and H. Morkoc, "Microwave Performance of AlGaN/GaN Inverted MODFETs," *IEEE Electron Device Letters*, vol. 18, pp. 293-295, 1997.

[20] Y.F. Wu, S. Keller, P. Kozodoy, B.P. Keller, P. Parikh, D. Kapolnek, S.P. Denbaars, and U.K. Mishra, "Bias Dependent Microwave Performance of AlGaN/GaN MODFETs Up to 100V, *IEEE Electron Device Letters*, vol. 18, pp. 290-292, 1997.

[21] A.T. Ping, M. A. Khan, Q. Chen, J.W. Yang, and I. Adesida, "Dependence of DC and RF Characteristics on Gate Length for High Current AlGaN/GaN HFETs," *Electronics Letters*, vol. 33, pp. 1081-1083, 1997.

[22] Z. Fan, C, Lu, A.E. Botchkarev, H. Tang, A. Salvador, O. Aktas, W. Kim, and H. Morkoc, "AlGaN/GaN Double Heterostructure Channel Modulation Doped Field Effect Transistors," *Electronics Letters*, vol. 33, pp. 814-815, 1997.

[23] J. Burm, K. Chu, W. J. Schaff, L. F. Eastman, A. M. Khan, Q. Chen, Y. J. W., and M. S. Shur, "0.12 mm Gate III-V Nitride HFET's With High Contact Resistances," *IEEE Electron Device Letters*, vol. 18, pp. 141-143, 1997.

[24] Q. Chen, R. Gaska, A. M. Khan, M. S. Shur, A. Ping, I. Adesida, J. Burm, W. J. Schaff, and L. F. Eastman, "Microwave Performance of 0.25 mm Doped Channel GaN/AlGaN Heterostructure Field Effect Transistor at Elevated Temperatures," *Electronics Letters*, vol. 33, pp. 637-638, 1997.

[25] Y.F. Wu, B.P. Keller, S. Keller, D. Kapolnek, S.P. Denbaars, and U.K. Mishra, "Measured Microwave Power Performance of alGaN/GaN MODFETs," *IEEE Electron Device Letters*, vol. 17, pp. 455-457, 1996.

[26] L. Eastman, K. Chu, W. Schaff, M. Murphy, N. Weinmann, and T. Eustis, "High Frequency AlGaN/GaN MODFETs," *MRS Internet Journal Nitride Semiconductor Research*, vol. 2, 1997.

[27] R. Gaska, J. W. Yang, A. Osinsky, A. D. Bykhovski, and M. S. Shur, "Piezoeffect and Gate Current in AlGaN/GaN High Electron Mobility Transistors," *Applied Physics Letters*, vol. 71, pp. 3673-3675, 1997.

[28] P. M. Asbeck, E. T. Yu, S. S. Lau, G. J. Sullivan, J. Van Hove, and J. Redwing, "Piezoelectric Charge Densities in AlGaN/GaN HFETs," *Electronics Letters*, vol. 33, pp. 1230-1231, 1997.

[29] R. Gaska, J. W. Yang, A. D. Bykhovski, and M. S. Shur, "Piezoresistive Effect in GaN-AlN-GaN Structures," *Applied Physics Letters*, vol. 71, pp. 3817-3819, 1997.

[30] R. Gaska, A. Osinsky, J. W. Yang, and M. S. Shur, "Self-Heating in High-Power AlGaN-GaN HFETs," *Electron Device Letters*, vol. 19, pp. 89-91, 1998.

[31] B. J. Thibeault, B. P. Keller, Y.-F. Wu, P. Fini, U. K. Mishra, C. Nguyen, N. X. Nguyen, and M. Le, "High Performance and Large Area Flip-Chip Bonded AlGaN/GaN MODFETs," presented at International Electron Devices Meeting, Washington DC, 1997.

[32] A.T. Ping, Q. Chen, J.W. Wang, M. A. Khan, and I. Adesida, "DC and Microwave Performance of High-Current AlGaN/GaN Heteostructure Field Effect Transistors Grown on p-Type SiC Substrates," *IEEE Electron Device Letters*, vol. 19, pp. 54-56, 1998.

[33] M. N. Yoder, "Wide Bandgap Semiconductor Materials and Devices," *IEEE Transactions on Electron Devices*, vol. 43, pp. 1633-1636, 1996.

[34] R.J. Trew, "The Operation of Microwave Power Amplifiers Fabricated From Wide Bandgap Semiconductors,", *1997 IEEE MTT-S Digest*, pp. 45-48, 1997.